Article

Brain morphometry and cognitive features in prediction of irritable bowel syndrome (v 20241126) Submission deadline (Diagnostics): 2024-11-30

Application of Artificial Intelligence in Gastrointestinal Disease https://www.mdpi.com/journal/diagnostics/special_issues/CS1956QYIM

Astri J. Lundervold [1] 0000-0002-6819-6164*, Ben René Bjørsvik [2], Julie Billing [1], Birgitte Berentsen [5,6] 0000-0003-3574-7078, Gülen Arslan Lied [5,6] 0000-0002-1827-5008, Elisabeth K Steinsvik [5] 0000-0002-8371-1988, Trygve Hausken [5] 0000-0001-7080-8396, [4‡], Daniela M. Pfabigan [1] 0000-0002-4043-1695, Arvid Lundervold [2,3‡] 0000-0002-0032-4182

1   Department of Biological and Medical Psychology, University of Bergen, Norway
2   Department of Biomedicine, University of Bergen, Bergen, Norway
3   Medical-AI, Mohn Medical Imaging and Visualization Center, Department of Radiology, Haukeland University Hospital, Bergen, Norway
4   Department of Clinical Medicine, University of Bergen, Bergen 5021, Norway
5   National Center for Functional Gastrointestinal Disorders, Department of Medicine, Haukeland University Hospital, Bergen 5021, Norway
6   Department of Biomedicine, University of Bergen, Bergen, Norway
5   Medical-AI, Mohn Medical Imaging and Visualization Center, Department of Radiology, Haukeland University Hospital, Bergen, Norway
*   Correspondence:Astri.Lundervold@uib.no

Abstract: *Background:* Irritable bowel syndrome (IBS) is a common condition within the spectrum of gut-brain disorders, characterized by abdominal pain, bloating, altered bowel habits, and different patterns of psychological distress. While brain-gut interactions are increasingly recognized in IBS pathophysiology, the relationship between brain morphometry, cognitive function, and clinical presentation remains poorly understood. *Objectives:* To investigate whether multivariate analysis of brain morphometric measures and cognitive test performance can distinguish patients with IBS from healthy controls (HCs), and to evaluate the relative importance of structural and cognitive features in this discrimination. *Methods:* In this cross-sectional study, 49 patients with IBS and 29 HCs underwent structural magnetic resonance imaging (MRI) brain examination and completed the Repeatable Battery for the Assessment of Neuropsychological Status (RBANS). Brain morphometry was analyzed using two versions of FreeSurfer software (v6.0.1 and v7.4.1). IBS severity was assessed using the IBS-Severity Scoring System (IBS-SSS). We employed both univariate and multivariate statistical and machine learning approaches, including cross-validation, to analyze morphometric and cognitive measures. *Results:* Univariate and multivariate analyses showed limited discrimination between IBS and HC groups using morphometric measures alone. However, when combining morphometric and cognitive measures in a machine learning framework, the model achieved 93% sensitivity in identifying IBS patients, albeit with 78% specificity. Feature importance analysis highlighted the significance of subcortical structures (particularly hippocampus, caudate, and putamen) and two cognitive domains (recall and verbal skills) in group discrimination. Software version comparison revealed substantial impact on morphometric measurements. *Conclusions:* Our findings suggest that the combination of brain morphometry and cognitive measures provides better discrimination between IBS and HC groups than either measure alone. The identified importance of subcortical structures and specific cognitive domains supports a complex brain-gut interaction in IBS. These results emphasize the need for multimodal approaches in IBS research and careful consideration of methodological factors in brain morphometry studies.

Keywords: Irritable bowel syndrome; structural MRI; brain morphometry, cognition; supervised classification; machine learning

Introduction

Irritable bowel syndrome (IBS) represents a prevalent and complex gastrointestinal (GI) disorder, affecting approximately 10% of the global population [1]. The syndrome is clinically defined by a characteristic symptom pattern: recurrent abdominal pain associated with defecation, accompanied by alterations in bowel habits [2], and can be divided into clinical phenotypes based on predominant bowel patterns [3] and overall symptom severity [4]. The clinical presentation is heterogeneous, with experiences ranging from mild discomfort to severe symptoms that substantially impair quality of life and daily functioning [4]. Notably, women are disproportionately affected, a difference that appears to arise from a complex interplay of biological factors (including hormonal influences), healthcare-seeking behaviors, and sociocultural determinants [5–8]. Such epidemiological patterns highlight the multifactorial nature of IBS and underscore the importance of considering both biological and psychosocial factors in its study and treatment.

A bidirectional relationship between gastrointestinal symptoms of IBS and psychological functioning is well-documented [9]. While gastrointestinal symptoms can trigger or exacerbate psychological distress, anxiety and depression may in turn amplify the intensity and frequency of abdomal pain [10]. Recent research has expanded this psychobiological framework to include cognitive function, revealing a more nuanced picture of brain-gut interactions in IBS. Although cognitive impairments have been demonstrated at the group level [11,12], these deficits seem to characterize specific subgroups rather than being a universal feature of IBS [9,13]. This heterogeneity in psychological and cognitive presentations aligns with contemporary models of the gut-brain axis [14,15], which conceptualize IBS as a disorder of disrupted neural-enteric communication. In these models, the brain serves as the central integration hub for processing and interpreting the complex array of visceral signals, emotional responses, and cognitive processes that may be involved in IBS.

The relationship between brain structure and cognitive function has evolved from simple localization models to more sophisticated network-based frameworks [16,17]. This network perspective gained particular relevance for understanding IBS through Mayer et al.'s [18] seminal paper in 2015, which proposed that alterations in brain networks could directly influence multiple cognitive domains in IBS patients. Recent empirical support for this systems-level approach comes from Li et al. [19], who identified several associations between symptom severity and regional brain volumes, including positive correlations with subcortical structures (globus pallidus, caudate, and putamen) and negative correlations with cortical regions (anterior cingulate, dorsolateral prefrontal cortex, anterior and mid-cingulate cortices) and subcortical areas (anterior insula, hippocampus, parahippocampal cortex, thalamus). Of special interest to the present study, they also showed that these brain regions were linked to cognitive performance on tests of language skills and memory function.

Studies of abdominal pain and visceral stimulation have consistently demonstrated involvement of distributed brain networks, encompassing both cortical and subcortical structures [20,21]. Building on this network perspective, Skrobisz et al. [22] conducted a comprehensive morphometric analysis in patients with non-specific digestive disorders, including IBS. Using FreeSurfer software (version 6.0.1), they analyzed 36 brain regions, including subcortical, cortical, and global measures derived from structural magnetic resonance imaging (MRI). Their univariate analyses revealed reduced thalamic volume in IBS patients compared to healthy controls, though volumes remained larger than in patients with inflammatory bowel diseases. While these findings suggest structural brain differences in IBS, univariate approaches may not capture the full complexity of brain-gut interactions. Therefore, our study builds upon Skrobisz et al.'s work in two key ways. First, we examine the robustness of their findings by comparing analyses using both FreeSurfer v6.0.1 and a more recent version, allowing us to differentiate between software-dependent and

true biological effects. Second, we extend beyond univariate analyses by implementing multivariate approaches, including supervised machine learning techniques, to capture complex patterns in brain morphometry that might better characterize IBS. This dual approach - methodological validation and advanced pattern analysis - aims to provide a more comprehensive understanding of the structural brain differences associated with IBS. Finally, responding to Skrobisz et al.'s [22] call for integrating clinical measures, we investigated whether combining cognitive performance data with morphometric features would enhance the accuracy of IBS versus HC classification.

We will address these aims in the following way:

A   We aim to replicate the morphometric differences between IBS patients and HC reported in [22] by using the same FreeSurfer software version (FS 6.0.1) and a similar univariate analysis approach as in the original study.

B   We will compare outcomes of the morphometric segmentation of the T1-w recordings in the current dataset ($n = 78$) for the FreeSurfer software version used in [22] (FS 6.0.1) with a more recent version (FS 7.4.1) by calculating pairwise correlations.

C   We will investigate if morphometric features (derived from the FS 7.4.1 brain segmentation) can be used to distinguish between IBS individuals and HC. To this end, we will employ four different strategies: (i) we will conduct univariate comparisons between IBS individuals and HC; (ii) we will conduct multivariate comparisons between the two groups (by incorporating covariance structures of the morphometric features; (iii) we will apply a machine learing framework (ML) to predict group membership based on morphometric features; and (iv) we will identify feature importance of respective morphometric features should the classification into IBS individuals and HC be successful.

D   We will investigate if the prediction of group membership (IBS vs. HC) is improved when cognitive performance is added as a predictor to the morphometric features ML model. If prediction is improved, we will identify those features that have the strongest influence on distinguishing IBS individuals from HC.

Materials and Methods

Participants

This investigation is part of the Bergen Brain-Gut project, a comprehensive clinical study conducted at Haukeland University Hospital, Norway, between 2020 and 2022 (detailed protocol in Berentsen et al. [23]). Our sample comprised 49 patients with IBS and 29 healthy controls (HCs), all aged 18 years or older. Participant recruitment employed multiple strategies, including media advertisements, informational flyers, and direct referrals from the hospital's outpatient clinic. All potential participants underwent systematic screening by a trained nurse using standardized inclusion and exclusion criteria (Table 1), followed by a comprehensive assessment battery including gastrointestinal measures, psychometric testing, and multiparametric magnetic resonance imaging (MRI).

The final sample size was determined by several factors. While no formal a priori power analysis was conducted as effect sizes for brain morphometric differences in IBS were not well established at the study's inception, our sample size aligns with or exceeds those of similar neuroimaging studies in functional gastrointestinal disorders [22]. For the current analyses, we included only participants with complete data on all key measures and artifact-free MRI scans suitable for automated brain segmentation, ensuring data quality while maintaining the largest possible sample size. This approach balanced statistical power requirements with practical constraints and methodological rigor.

Measures

Age and sex (not genetically verified) were self-reported by the participants at baseline.

Inclusion criteria	Exclusion criteria
Rome-IV criteria: Recurrent abdominal pain average at least 1 day/week during the last 3 and months, and associated alterations in bowel habits at least 6 months before diagnosis. Other causes are excluded.	Pharmacological treatment affecting GI tract, including medication for anxiety and depression, diabetes, coeliac disease, IBS, Polycystic ovary syndrome, active Helicobacter pylori infection, Parkinson's disease, amyotrophic lateral sclerosis, or Psychiatric disorders.
Normal diet at least 3 weeks before inclusion IBS score equal to or above 175	Treated with antibiotics for the last 3 months Diets such as vegetarian or vegan Use of probiotics or low-FODMAP diet within the last 3 weeks Previous intestinal surgery, except appendectomy Metallic implants, claustrophobia, incompatible with MRI Travel outside Europe last 3 weeks Plan to travel in the near future Pregnancy

Table 1. Exclusion and inclusion criteria for the IBS patients. Source: Retrieved from [23]

The IBS-Severity Scoring system (IBS-SSS)

The IBS-Severity Scoring system is a questionnaire used to assess the severity of GI-related IBS symptoms [24]. The questionnaire includes five items related to abdominal pain, distention, bowel habits, and quality of life. The maximum score for each question is 100. A sum of scores < 75 is used to define "no or minimal problems", and the scores in the ranges $[75, 175)$, $[175, 300]$, and > 300 as "mild", "moderate", and "severe" IBS symptoms, respectively [24]. In the present study, an IBS-SSS score ≥ 175 was used as the inclusion criteria for the IBS group. Almost all HCs obtained an IBS-SSS score at the lowest level (< 75), with some reporting a score within the mild level ($[75, 175)$).

Repeatable Battery for the Assessment of Neuropsychological Status (RBANS)

All participants performed the Norwegian A version of RBANS, administrated by a nurse trained by a clinical neuropsychologist, following the test manual's instructions [25]. The test battery comprises 10 subtests, which are combined into five index scores and a total score. These scores are expressed both as raw and as age-corrected scaled scores. The scaled scores have a mean value of 100 and a standard deviation of 15 and are based on performance in a normative group matched to population statistics of 2012 in Norway, Sweden, and Denmark. We used these scaled scores on each of the five RBANS indices for a pairwise correlation analysis between brain morphometric measures and cognitive performance.

MRI Data Acquisition

All neuroimaging data were acquired using a 3 Tesla Siemens Biograph mMR PET/MRI scanner equipped with a standard 12-channel head coil. The comprehensive multiparametric imaging protocol consisted of five sequences: a 3D T1-weighted MPRAGE (TA = 5:35), T2-weighted structural imaging (TA = 5:12), gradient echo (GRE) field mapping (TA = 0:54), resting-state functional MRI using echo-planar imaging (EPI) with integrated motion correction (TA = 9:48), and diffusion-weighted imaging with 30 gradient directions and three b-values (TA = 8:34). The total examination time was approximately 45 minutes. For the current morphometric analyses, we utilized only the high-resolution T1-weighted images, acquired using a 3D MPRAGE (Magnetization Prepared Rapid Gradient Echo) sequence. The acquisition parameters included a spatial resolution of 1.0 mm isotropic ($1 \times 1 \times 1$ mm^3) across 192 sagittal slices, with repetition time (TR) of 2500 ms, echo time (TE) of 2.26 ms, and inversion time (TI) of 900 ms. The field of view (FOV) was set to

256×256 mm^2 with a corresponding matrix size of 256×256, and parallel imaging was employed using GRAPPA with an acceleration factor of 2.

Figure 1 shows a representative T1-weighted image from our dataset, demonstrating the high tissue contrast necessary for accurate morphometric analysis. The corresponding FreeSurfer-generated segmentation mask, which forms the basis for our morphometric measurements, is illustrated in Figure 2. These images exemplify the quality standards maintained throughout our dataset.
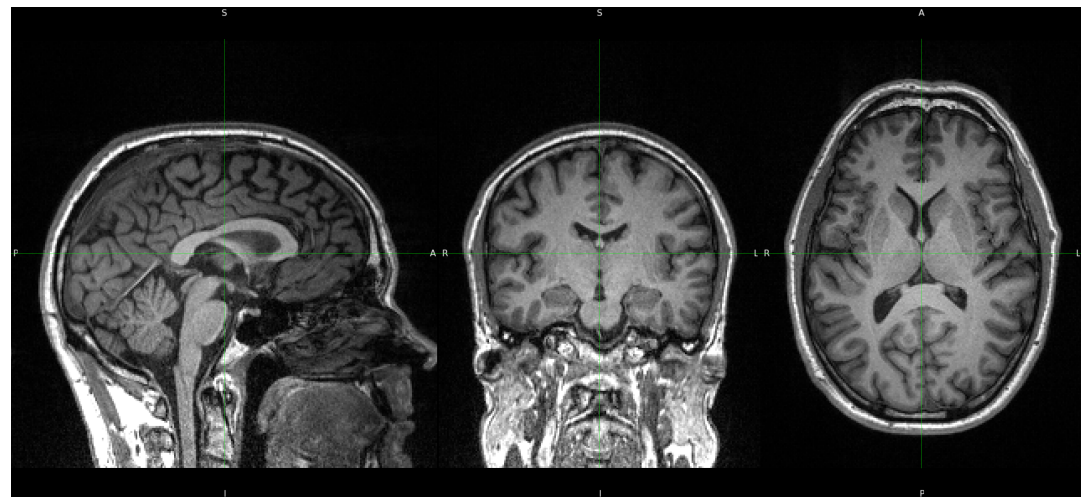
Figure 1. *3D T1-weighted MPRAGE recording from BGA_046.* Panels left to right: Sagittal, Coronal, and Axial section, respectively. (`01-freesurfer-freeview-t1-aseg-bga-046.ipynb`)
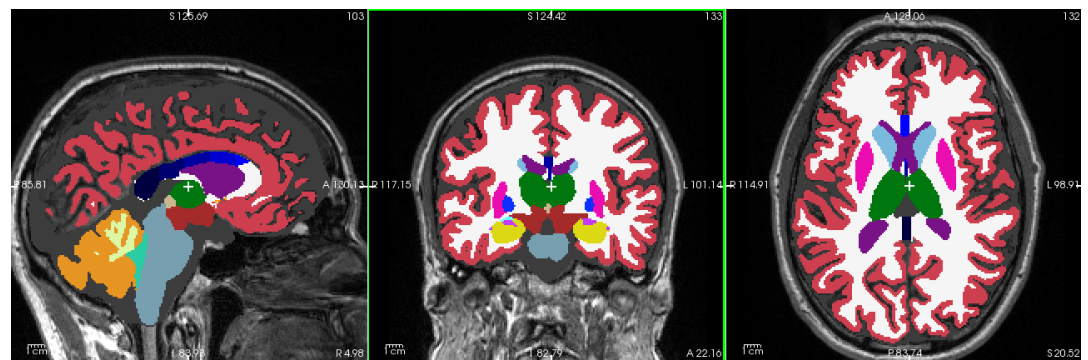
Figure 2. *The color-coded ASEG segmentation mask by FreeSurfer 7.4.1 overlaid on 3D T1-w MPRAGE from BGA_046.* Panels left to right: Sagittal, Coronal, Axial section, respectively. The white cross is located in the medial part of Left-Thalamus. Thalamus: green, Hippocampus: yellow, Caudate: light blue, Putamen: pink, Pallidum: purple, Cortex: red, White-Matter: white.

Brain Morphometry Analysis using FreeSurfer

Image processing and morphometric analyses were performed using FreeSurfer (https://freesurfer.net), a widely-validated open-source software suite for analyzing brain MRI data [26]. To address both methodological and biological questions, we conducted parallel analyses using two FreeSurfer versions: version 6.0.1, which was employed in the reference study by Skrobisz et al. [22], and the current version 7.4.1.

The evolution of FreeSurfer's capabilities is particularly relevant to our investigation of brain structure in IBS. Version 7.0 (July 2020) introduced significant improvements in subcortical segmentation accuracy, while version 7.4.1 (June 2023) further enhanced the precision of limbic system structures, notably the hippocampus and amygdala. Additionally, version 7.4.1 provides superior compatibility with multi-modal imaging data and

implements refined longitudinal processing algorithms, though these capabilities were not utilized in the current cross-sectional study.

For both versions, we focused on the automated segmentation of subcortical structures using FreeSurfer's `aseg` pipeline, which identifies and quantifies the volume of distinct brain regions (detailed in Table A1). This dual-version approach serves two purposes: first, it enables direct comparison with Skrobisz et al.'s [22] findings, and second, it allows us to assess the impact of software evolution on morphometric measurements. This methodological consideration is crucial, as previous studies have demonstrated that version-dependent variations in automated segmentation can significantly influence morphometric results [27–32].

The enhanced accuracy of version 7.4.1 is particularly relevant for our investigation of IBS, as it provides more reliable quantification of brain regions implicated in visceral sensation, pain processing, emotional regulation, and cognitive function. However, by analyzing our data with both versions, we can distinguish between genuine biological differences and methodologically-induced variations in brain morphometry.

Statistical and Machine Learning Analysis

All analyses were implemented in Python (version 3.10), with complete computational workflows and reproducibility materials available in our public GitHub repository (https://arvidl.github.com/ibs-brain). Our analytical approach combined traditional statistical methods with advanced machine learning techniques, employing both parametric and non-parametric approaches as appropriate for the data distributions.

For group comparisons, statistical significance was assessed using a threshold of $p < 0.05$, with Bonferroni correction applied to control for multiple comparisons. Effect sizes were quantified using Cliff's Delta, a robust non-parametric measure particularly suitable for non-normally distributed data. Following established conventions, we interpreted Cliff's Delta values as negligible (0.00-0.14), small (0.15-0.33), medium (0.34-0.47), or large (0.48-1.00).

Relationships between variables were evaluated using Spearman's rank correlation coefficient (ρ), chosen for its robustness to non-normality and ability to capture monotonic relationships. Correlation strengths were classified as weak (0.20-0.39), moderate (0.40-0.59), strong (0.60-0.79), or very strong (0.80-1.00). Values below 0.20 were considered negligible to minimize the risk of over-interpreting weak associations.

To ensure reproducibility and transparency, all analysis scripts, including data preprocessing steps, statistical analyses, and visualization code, are documented in Jupyter notebooks accessible through our GitHub repository. These notebooks provide detailed documentation of parameter choices, statistical assumptions, and analytical decisions.

Our analysis strategy addressed four interconnected research objectives, progressing from replication to more advanced multivariate approaches:

Research Objectives and Analytical Approach

A - Replication Analysis :

Is it possible to replicate the morphometric findings in Skrobisz et al. [22] regarding IBS vs. HC, using the same FreSurfer-derived features and the same FreeSurfer version?

(i) By employing a feature-by-feature (univariate) comparison?

B - Software Version Comparison :

Are there differences in morphometric feature values between FreeSurfer 6.0.1 and FreeSurfer 7.4.1 applied to the same set ($n = 78$) of 3D T1-w recordings in our cohort?

(i) By employing a feature-by-feature comparison?

(ii) Employing a multivariate comparison, incorporating covariance structures in the morphometric features?

C - Morphometric Classification Analysis :

Is it possible to separate IBS individuals from HC based on morphometric features?

(i) By employing a feature-by-feature comparison (FS 7.4.1)?

(ii) Employing a multivariate comparison, incorporating covariance structures in the morphometric features?

(iii) By predicting IBS vs. HC from the morphometric features using a machine learning framework (ML)?

(iv) identifying feature importance of the morphometric measures in the model with the best prediction?

D - Integrated Morphometric-Cognitive Analysis :

Would adding cognitive performance as a predictor improve the accuracy of separating IBS from HC?

(i) By employing a feature-by-feature comparison?

(ii) Employing a multivariate comparison, incorporating covariance structures in the cognitive features?

(iii) By predicting IBS vs. HC from the morphometric and cognitive features using a machine learning framework (ML)?

(iv) identifying feature importance of the morphometric and cognitive measures included in the model with the best prediction?

This hierarchical analytical framework progresses from basic replication to more advanced multivariate approaches, enabling both methodological validation and novel insights into IBS-related brain structure and function.

Statistical Analysis Framework

Given the complexity of our research questions and the combination of traditional and advanced analytical methods, we implemented a comprehensive statistical framework encompassing both univariate and multivariate approaches. Here we detail our analytical strategy and its methodological justification.

Exploratory and Univariate Analyses

Initial analyses followed established protocols [22], beginning with exploratory data analysis of numerical features and cross-tabulation of categorical variables (Group: HC/IBS; Sex: F/M). For univariate comparisons (Objectives A-D), we employed both parametric (independent t-tests) and non-parametric (Mann-Whitney U) tests, depending on normality assessments. Multiple comparison correction used the Bonferroni method, and effect sizes were quantified using both Cohen's d (for parametric tests) and Cliff's delta (for non-parametric analyses).

Permutation Testing

To address the challenges of small sample sizes and potential non-normal distributions, we implemented permutation testing with 1,000 iterations. This approach calculates an observed test statistic (sum of squared differences between group means) and generates a null distribution by randomly reassigning group labels and recalculating the statistic. The resulting empirical p-value represents the proportion of permuted statistics exceeding the observed value. This method offers several advantages: robustness to non-normality, natural handling of multiple comparisons, and suitability for small samples in multivariate analyses.

Multivariate Approaches

For multivariate analyses (Objectives B-D), we first assessed multivariate normality using two complementary methods: Mardia's test (examining skewness and kurtosis) and the more comprehensive Henze-Zirkler's test, both implemented in SciPy's stats module. Effect sizes were quantified using Partial η^2 (Eta-squared), interpreted following established guidelines [33]: small $(0.01 - 0.06)$, medium $(0.06 - 0.14)$, and large (≥ 0.14) effects.

Advanced Distance Metrics

To capture the complexity of high-dimensional relationships, we employed the Generalized Mahalanobis distance [34]. This sophisticated metric accounts for the covariance structure of the data while maintaining scale invariance across features. The method employs Moore-Penrose pseudoinversion to handle near-singular covariance matrices, enabling robust analysis even with highly correlated features. Significance can be assessed either parametrically through chi-square distribution or non-parametrically via permutation testing, providing flexibility in statistical inference. While this metric assumes similar covariance structures between groups, we supplemented it with permutation testing when this assumption was potentially violated. The combination of these approaches ensures robust statistical inference while acknowledging the inherent complexity of brain morphometry data.

Prediction of class belonging using machine learning

In tasks **C(iii)** - **D(iii)** we applied a comprehensive machine learning framework, utilizing morphometric features derived from FreeSurfer (`aseg`) to develop predictive models for two distinct classification tasks. We employed *PyCaret* (https://pycaret.org), an open-source, low-code machine learning library in Python, to develop and evaluate our classification models.

Machine Learning Model Development

Our machine learning approach followed a systematic protocol designed to ensure robust classification while addressing the challenges of limited sample size and potential overfitting. The analysis pipeline consisted of several carefully constructed stages optimized for neuroimaging data classification.

Initial data preparation employed a stratified sampling approach, partitioning the dataset into training (70%) and testing (30%) sets while preserving the distribution of key variables (IBS/HC status, sex, and cognitive function levels) across both partitions. This stratification was crucial for maintaining representative samples and ensuring valid model evaluation, particularly given our modest sample size and the inherent complexity of neuroimaging data.

Model development utilized PyCaret's comprehensive machine learning framework to evaluate multiple classification algorithms, ranging from traditional approaches to advanced ensemble methods. The classifier suite included linear models (Logistic Regression with L1 and L2 regularization), non-linear algorithms (Support Vector Machines (SVM) with various kernels), tree-based methods (Random Forests, Gradient Boosting Machines including XGBoost and LightGBM), and instance-based learners (K-Nearest Neighbors). This diverse algorithm selection enabled exploration of different decision boundaries and feature interaction patterns.

To ensure robust model assessment and mitigate overfitting risks, we implemented a nested cross-validation strategy. The outer loop employed 10-fold cross-validation for model selection, while the inner loop optimized hyperparameters through random search with internal cross-validation. This approach provided unbiased performance estimates while preventing data leakage between model selection and evaluation phases. Hyperparameter optimization focused on algorithm-specific parameters crucial for neuroimaging data: regularization strengths for linear models, kernel parameters for SVMs, tree structure parameters for ensemble methods, and neighborhood configurations for instance-based

learners. The final model selection prioritized both predictive performance and model interpretability, considering the clinical relevance of our findings.

Model Performance Assessment

Model evaluation employed a multi-faceted approach to ensure comprehensive performance assessment, particularly important given our class imbalance between IBS and HC groups. While overall classification accuracy provided an initial performance indicator, we implemented additional metrics to capture nuanced aspects of model behavior and clinical relevance.

Our primary evaluation framework combined complementary performance measures. The F1 score, computed as the harmonic mean of precision and recall, offered a balanced assessment of model performance by considering both false positives and false negatives. We supplemented this with the Receiver Operating Characteristic Area Under Curve (ROC-AUC), which quantifies discrimination ability across different classification thresholds and is particularly robust to class imbalance. For detailed error analysis, we generated confusion matrices showing the distribution of correct and incorrect predictions across classes, enabling identification of specific classification patterns and potential biases.

For the cognitive function analysis, which involved multiple classes, we employed macro-averaged versions of all metrics. This approach, calculating metrics independently for each class before averaging, ensures equal weighting of all classes regardless of their relative frequencies in the dataset. This consideration was particularly crucial given the uneven distribution of cognitive performance levels in our sample.

Performance assessment followed a dual-track strategy, evaluating models on both cross-validated training data and the held-out test set. This approach enabled us to assess both learning capacity and generalization ability, crucial considerations for clinical applications. To quantify uncertainty in our performance estimates, we calculated 95% confidence intervals for all metrics using bootstrapping methods. These intervals provide important context for interpreting model reliability and potential clinical utility, particularly given our moderate sample size.

The comprehensive evaluation strategy, combining multiple performance metrics with detailed error analysis and uncertainty quantification, ensures a thorough understanding of model behavior and reliability. This approach is particularly valuable for potential clinical applications, where understanding both model capabilities and limitations is crucial for responsible implementation.

Feature Importance and Model Interpretability Analysis

Understanding the relative contribution of different morphometric features to classification performance is crucial for both methodological validation and biological insight. We implemented two complementary approaches to feature importance analysis, combining model-agnostic methods with sophisticated game-theoretic interpretability techniques.

The first approach employed permutation importance analysis, which quantifies feature relevance by measuring the degradation in model performance when individual features are randomly permuted. For each morphometric feature, we performed multiple permutation iterations, calculating the mean decrease in model performance. This approach provides an intuitive measure of feature importance while remaining independent of the underlying model architecture, enabling consistent interpretation across different classification algorithms.

Our second approach utilized SHAP (SHapley Additive exPlanations) values, grounded in cooperative game theory [35]. This method offers a unified framework for model interpretation at both global and local levels. Global analysis aggregates SHAP values across all cases to identify consistently important features, while local analysis examines feature contributions to individual predictions. This dual-scale interpretation provides

crucial insights into how different brain regions contribute to classification decisions, both at the population level and for individual cases.

We applied both analytical approaches to our highest-performing models across all classification tasks. The results were synthesized through comprehensive visualization techniques, including SHAP summary plots depicting feature value distributions and their associated impact on model predictions. These visualizations integrate both the magnitude and directionality of feature effects, providing insight into how specific morphometric characteristics influence classification decisions.

The integration of permutation importance and SHAP analysis provides complementary perspectives on feature relevance. While permutation importance identifies features whose disruption most impacts model performance, SHAP analysis reveals the complex interactions between features and their contributions to specific predictions. This comprehensive approach to model interpretation enhances our understanding of the neurobiological features distinguishing IBS patients from healthy controls, while also illuminating potential relationships between brain structure, sex/gender differences, and cognitive function. The results not only validate our modeling approach but also suggest specific brain regions and networks that may play key roles in IBS pathophysiology.

Results

Sample Demographics and Clinical Characteristics

Our study included 78 participants (49 IBS patients and 29 healthy controls), with demographic and clinical characteristics summarized in Table 2. The age distributions were comparable between groups, with median ages of 34 years in the IBS group and 33 in the healthy control group. Both groups showed a predominance of female participants, with slightly higher representation in the IBS group (38 of 49) compared to the control group (20 of 29).

IBS symptom severity, assessed using the IBS-SSS, demonstrated clear group separation. The IBS group reported substantially higher symptom severity compared to healthy controls, consistent with our inclusion criteria. Missing IBS-SSS data for three participants in each group (total n = 6) were handled through multiple imputation. The observed severity scores in the IBS group indicate predominantly moderate to severe symptomatology, while healthy controls showed minimal gastrointestinal symptoms, as expected.

Group	Age Median (IQR)	IBS_SSS Median (IQR)	Sex F/M (%)	N	Missing IBS_SSS
HC (N=29)	33.0 (23.0)	21.0 (30.0)	69.0/31.0	29	3
IBS (N=49)	34.0 (14.0)	264.0 (95.0)	77.6/22.4	49	3

Table 2. Demographic and Clinical Characteristics of the Study Sample. Age is reported in years; IBS-SSS scores range from 0-500, with higher scores indicating greater symptom severity. IQR = Interquartile Range; F/M = Female/Male ratio expressed as percentages.

Table 3. Comparison of eTIV-normalized regional brain volumes between cohorts.

| Brain Region | Skrobisz Cohort (FS 6.0) | | | | Bergen Cohort (FS 6.0.1) | | | |
| | HC (N=19) | | IBS (N=20) | | HC (N=29) | | IBS (N=49) | |
	Mean	SD	Mean	SD	Mean	SD	Mean	SD
Left-Cerebellum-WM	0.00992	0.00113	0.00971	0.00107	0.01050	0.00092	0.01048	0.00092
Left-Cerebellum-Cortex	0.03628	0.00302	0.03553	0.00256	0.03894	0.00344	0.03931	0.00373
Left-Thalamus	0.00511	0.00037	0.00500	0.00024	0.00523	0.00046	0.00514	0.00039
Left-Caudate	0.00239	0.00025	0.00228	0.00021	0.00236	0.00026	0.00236	0.00031
Left-Putamen	0.00336	0.00033	0.00324	0.00028	0.00348	0.00038	0.00344	0.00039
Left-Pallidum	0.00140	0.00012	0.00135	0.00010	0.00140	0.00015	0.00137	0.00011
Left-Hippocampus	0.00270	0.00021	0.00272	0.00020	0.00291	0.00027	0.00290	0.00024
Left-Amygdala	0.00118	0.00013	0.00113	0.00015	0.00122	0.00010	0.00120	0.00010
Left-Accumbens-area	0.00031	0.00005	0.00034	0.00006	0.00043	0.00007	0.00042	0.00006
CSF	0.00061	0.00009	0.00060	0.00012	0.00067	0.00012	0.00070	0.00014
Right-Cerebellum-WM	0.00908	0.00106	0.00922	0.00100	0.00997	0.00089	0.00998	0.00085
Right-Cerebellum-Cortex	0.03652	0.00321	0.03616	0.00264	0.03972	0.00344	0.03998	0.00376
Right-Thalamus	0.00488	0.00030	0.00475	0.00024	0.00512	0.00044	0.00507	0.00036
Right-Caudate	0.00244	0.00024	0.00236	0.00024	0.00244	0.00024	0.00244	0.00030
Right-Putamen	0.00336	0.00030	0.00330	0.00028	0.00351	0.00037	0.00349	0.00035
Right-Pallidum	0.00136	0.00012	0.00133	0.00010	0.00132	0.00013	0.00130	0.00011
Right-Hippocampus	0.00282	0.00022	0.00285	0.00021	0.00301	0.00024	0.00298	0.00023
Right-Amygdala	0.00125	0.00012	0.00120	0.00012	0.00128	0.00009	0.00127	0.00010
Right-Accumbens-area	0.00034	0.00004	0.00036	0.00005	0.00043	0.00005	0.00043	0.00006
WM-hypointensities	0.00047	0.00015	0.00048	0.00013	0.00079	0.00031	0.00069	0.00025
CC_Posterior	0.00065	0.00013	0.00065	0.00010	0.00065	0.00010	0.00070	0.00011
CC_Mid_Posterior	0.00038	0.00007	0.00036	0.00007	0.00037	0.00007	0.00040	0.00007
CC_Central	0.00039	0.00009	0.00043	0.00008	0.00039	0.00009	0.00039	0.00010
CC_Mid_Anterior	0.00041	0.00009	0.00044	0.00013	0.00038	0.00008	0.00041	0.00011
CC_Anterior	0.00062	0.00010	0.00061	0.00008	0.00062	0.00010	0.00065	0.00010
BrainSegVol	0.75340	0.01784	0.74913	0.01647	0.80464	0.02487	0.80558	0.02397
BrainSegVolNotVent	0.74137	0.01880	0.73857	0.01836	0.79224	0.02511	0.79132	0.02490
lhCortexVol	0.15339	0.00620	0.15313	0.00871	0.16670	0.00800	0.16693	0.00951
rhCortexVol	0.15490	0.00690	0.15467	0.00859	0.16614	0.00828	0.16646	0.00939
CortexVol	0.30829	0.01298	0.30780	0.01715	0.33283	0.01611	0.33339	0.01880
lhCerebralWhiteMatterVol	0.15101	0.00748	0.15058	0.00742	0.15990	0.00858	0.15915	0.00876
rhCerebralWhiteMatterVol	0.15103	0.00757	0.15075	0.00727	0.15925	0.00829	0.15827	0.00938
CerebralWhiteMatterVol	0.30205	0.01500	0.30133	0.01461	0.31915	0.01678	0.31742	0.01808
SubCortGrayVol	0.03930	0.00194	0.03855	0.00162	0.04092	0.00258	0.04063	0.00236
TotalGrayVol	0.42105	0.01376	0.41884	0.01868	0.45307	0.02208	0.45396	0.02432

HC = Healthy Controls; IBS = Irritable Bowel Syndrome; SD = Standard Deviation.
All volumes are normalized to estimated total intracranial volume (eTIV).

Univariate comparisons between HC and IBS: FSv 6.0.1 and FSv7.4.1   419

Table 3 shows the mean and standard deviation on each of the included morphometric   420
measures. Non-parametric tests with Bonferroni correction showed no statistically sig-   421
nificant differences between the HC and the IBS group, neither when analysed with FS   422
6.0.1 nor with FS 7.4.1 (A2 and A3). Without the Bonferroni correction, we find a trend   423
($p < .05$) for the morphometric measure of hypointensities and the posterior part of the   424
corpus callosum, but only when analysed with the FS 6.0.1 software version. With large   425
and widespread differences when comparing the results with FS 6.0.1 versus FS 7.4.1 (Table 426
5 and 6, and Figure A1), these findings, and probably also the finding in Skrobiz et al.'s   427
paper [22], represent software differences rather than biological differences.   428

Table 4. Table tab:brain-regions-full: Comparison of Brain Region Volumes in IBS Patients and Healthy Controls

Brain Region	FS 6.0.1				FS 7.4.1			
	HC (N=29)		IBS (N=49)		HC (N=29)		IBS (N=49)	
	Mean	SD	Mean	SD	Mean	SD	Mean	SD
Left-Lateral-Ventricle	0.004770	0.002111	0.005654	0.003821	0.004715	0.001998	0.005529	0.003566
Right-Lateral-Ventricle	0.004587	0.002091	0.005373	0.003389	0.004518	0.002072	0.005223	0.003243
Left-Inf-Lat-Vent	0.000189	0.000085	0.000210	0.000094	0.000183	0.000078	0.000187	0.000077
Right-Inf-Lat-Vent	0.000202	0.000095	0.000208	0.000114	0.000200	0.000086	0.000209	0.000104
Left-Cerebellum-White-Matter	0.010496	0.000900	0.010483	0.000915	0.010603	0.000916	0.010607	0.001016
Right-Cerebellum-White-Matter	0.009973	0.000875	0.009979	0.000842	0.010052	0.000918	0.010108	0.001005
Left-Cerebellum-Cortex	0.038939	0.003375	0.039314	0.003695	0.038066	0.003465	0.038056	0.003646
Right-Cerebellum-Cortex	0.039719	0.003385	0.039978	0.003721	0.038881	0.003472	0.038912	0.003635
Left-Thalamus	0.005232	0.000456	0.005144	0.000389	0.005236	0.000513	0.005114	0.000453
Right-Thalamus	0.005120	0.000431	0.005071	0.000354	0.005190	0.000447	0.005053	0.000409
Left-Caudate	0.002356	0.000254	0.002355	0.000303	0.002346	0.000279	0.002317	0.000291
Right-Caudate	0.002438	0.000235	0.002439	0.000298	0.002418	0.000281	0.002402	0.000283
Left-Putamen	0.003479	0.000378	0.003441	0.000382	0.003438	0.000389	0.003370	0.000325
Right-Putamen	0.003506	0.000359	0.003489	0.000348	0.003487	0.000395	0.003466	0.000319
Left-Pallidum	0.001405	0.000151	0.001374	0.000106	0.001380	0.000134	0.001358	0.000094
Right-Pallidum	0.001323	0.000124	0.001301	0.000106	0.001321	0.000135	0.001306	0.000117
Left-Hippocampus	0.002913	0.000268	0.002896	0.000240	0.002926	0.000247	0.002895	0.000241
Right-Hippocampus	0.003013	0.000236	0.002983	0.000227	0.003049	0.000226	0.002986	0.000233
Left-Amygdala	0.001218	0.000095	0.001203	0.000104	0.001228	0.000131	0.001190	0.000109
Right-Amygdala	0.001284	0.000085	0.001271	0.000097	0.001269	0.000105	0.001260	0.000104
Left-Accumbens	0.000427	0.000068	0.000421	0.000057	0.000424	0.000060	0.000400	0.000056
Right-Accumbens	0.000428	0.000052	0.000427	0.000060	0.000434	0.000053	0.000435	0.000057
Left-VentralDC	0.002817	0.000211	0.002822	0.000197	0.002763	0.000169	0.002722	0.000205
Right-VentralDC	0.002772	0.000193	0.002796	0.000210	0.002761	0.000175	0.002746	0.000221
Left-vessel	0.000021	0.000013	0.000020	0.000015	0.000021	0.000012	0.000020	0.000015
Right-vessel	0.000017	0.000012	0.000019	0.000016	0.000013	0.000008	0.000016	0.000016
Left-choroid-plexus	0.000324	0.000091	0.000343	0.000107	0.000323	0.000098	0.000329	0.000108
Right-choroid-plexus	0.000353	0.000096	0.000368	0.000111	0.000352	0.000098	0.000365	0.000106
3rd-Ventricle	0.000674	0.000169	0.000702	0.000218	0.000668	0.000168	0.000688	0.000205
4th-Ventricle	0.001209	0.000310	0.001244	0.000333	0.001152	0.000318	0.001178	0.000311
Brain-Stem	0.014544	0.000969	0.014610	0.000896	0.014253	0.000800	0.014172	0.000928
CSF	0.000670	0.000118	0.000702	0.000140	0.000658	0.000112	0.000689	0.000128
WM-hypointensities	0.000791	0.000300	0.000688	0.000250	0.000787	0.000472	0.000667	0.000242
Optic-Chiasm	0.000103	0.000025	0.000119	0.000031	0.000089	0.000038	0.000095	0.000033
$CC_{posterior}$	0.000652	0.000095	0.000702	0.000111	0.000645	0.000094	0.000685	0.000112
$CC_{MidPosterior}$	0.000369	0.000065	0.000401	0.000071	0.000366	0.000067	0.000394	0.000073
$CC_{Central}$	0.000395	0.000087	0.000391	0.000104	0.000390	0.000090	0.000390	0.000100
$CC_{MidAnterior}$	0.000379	0.000080	0.000409	0.000112	0.000384	0.000076	0.000400	0.000104
$CC_{Anterior}$	0.000623	0.000094	0.000650	0.000099	0.000608	0.000096	0.000646	0.000111

Note: All volumes are normalized to estimated total intracranial volume (eTIV).

HC = Healthy Controls; IBS = Irritable Bowel Syndrome Group; SD = Standard Deviation.

Generated in `compare_FSversions.ipynb`

Multivariate analyses: IBS versus HC

A generalized Mahalanobis distance, a partial η^2 (Eta-squared), and a permutation test were computed to reveal how distinct the two groups (IBS and HC) are in a multidimensional space. Analog to the univariate analyses, no significant differences were observed: general Mahalanobis distance (= 2.0427), Partial η^2 (= 0.013), the permutation test (p = .45 (4515). From a clinical perspective, these results indicate that the brain morphometry of IBS patients, as measured by these variables, does not differ substantially from that of healthy controls.

Prediction of IBS versus HC from morphometric measures

A large set of machine learning models were trained on a data set including 54 participants (43 women), of which 34 belonged to the IBS group. Among the 24 participants allocated to the test data set (15 women), 15 participants were from the IBS group.

Gradient Boosting (xgboost) was selected as the best model, with an accuracy of 0.7200 in the train-set, with a reduction (accuracy = 0.5000) in the test set. The confusion matrix, Figure 3 (a) shows that the majority of the IBS patients in the test set (73%) were correctly classified (11/15), while all but one HC was misclassified as IBS. The misclassified IBS

patients were somewhat older than the correctly classified patients, with a higher and more distributed IBS-SSS score.

3 (b) shows the features with the strongest importance. Among the top ten features we find different parts of the corpus callosum and subcortical structures like Accumbens, Amygdala, Pallidum and Hippocampus, but also more global measures like the eTIV.
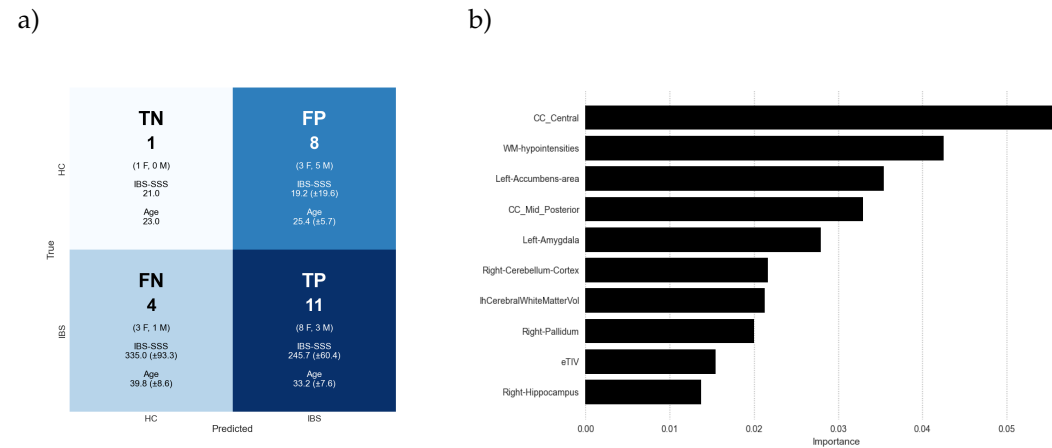

Figure 3. (a) Confusion matrix (XGBOOST) predicting IBS versus HC from brain morphometry.TN = true negative, FP = false positive, FN = false negative, TP = true positive. (b) Top 10 feature importance with Group (IBS vs HC) as the outcome variable and morphometric features as predictors.

Figure 4. SHAP values with morhometry as predictors

Note:X-axis (SHAP values): The SHAP values indicate the impact each feature has on the model's output, which is the probability of classifying someone as IBS patient or HC. Values to the right of 0 indicate a positive contribution (towards one class, likely HCs in this case). Values to the left indicate a negative contribution (likely towards IBS). Color gradient (Feature Value): This represents the actual feature value: Red/pink indicates a high feature value. Blue/purple indicates a low feature value.

Figure 4 shows SHAP values, which measure how different brain regions impact a predictive model's output. The right-hemispheric structures (caudate, hippocampus) appear most

important for whatever outcome the model is predicting, suggesting these areas might deserve particular attention in patient assessment. There is also a pattern suggesting the basal ganglia network as a whole as important for the model's predictions, with right-hemispheric structures (especially caudate) showing stronger effects than left-hemispheric ones. Other subcortical structures like the amygdala and hippocampus also show notable effects, supporting a broader subcortical involvement in predicting IBS versus HC.

Univariate analysis of the cognitive features

Table 4 shows that the HC group obtained significantly higher scores on the full-scale RBANS measure, with a medium effect size. Non-parametric comparisons were used to account for non-normality distributions. Scores for the Visuospatial Index and the Attention Index were non-significant, with negligible effect sizes. For the two memory indexes, the Immediate Memory and Recall Indexes, the HC group scored significantly higher than the IBS group. Statistical significance was observed after Bonferroni correction solely for the Recall index, where Cliffs delta indicated a small effect size.

Variable	HC	IBS	p-value	Cliff's delta
Fullscale_RBANS	103.0 (93.0-108.0)	91.0 (85.0-100.0)	0.002	0.213
Memory_Index	100.0 (86.0-109.0)	86.0 (81.0-105.0)	0.031	0.147
Visuoaspatial_Index	97.0 (90.0-107.0)	96.0 (90.0-105.0)	0.763	0.021
Verbal skills Index	105.0 (95.0-113.0)	95.0 (89.0-111.0)	0.087	0.116
Attention_Index	98.0 (89.0-108.0)	97.0 (83.0-101.0)	0.118	0.107
Recall_Index	107.0 (92.0-113.0)	95.0 (85.0-100.0)	0.006	0.186

Table 5. A non-parametric analysis comparing cognitive features in the IBS and HC groups. Cliff's delta is used to estimate effect sizes.

Correlations between morphometric and cognitive features

Figure 5 shows a heatmap to illustrate the pairwise correlations between the included morphometric volume measures, the RBANS indexes, and the Fullscale RBANS score. The correlations between the Fullscale score and each of the five indexes are moderate to strong for all expect the Verbal skills index. Furthermore, there is a strong correlation between the two memory scores (Immediate memory and Recall).The strongest correlations between RBANS and the morphometric measures were found between the Recall index and subcortical structures like hippocampus, amygdala and accumbens, but these correlations should still be defined as weak. The strongest correlation (r = .33) was found between white matter hypointensities and the Visuospatial index. Most of the correlations between subcortical strucures were moderate, with some very strong correlations between structures on the left and right hemisphere (e.g., Putamen r_s = .95; Caudate r_s = .94; Thalamus r_s =.90; Hippocampus r_s = .82 and Pallidum r_s = .78).
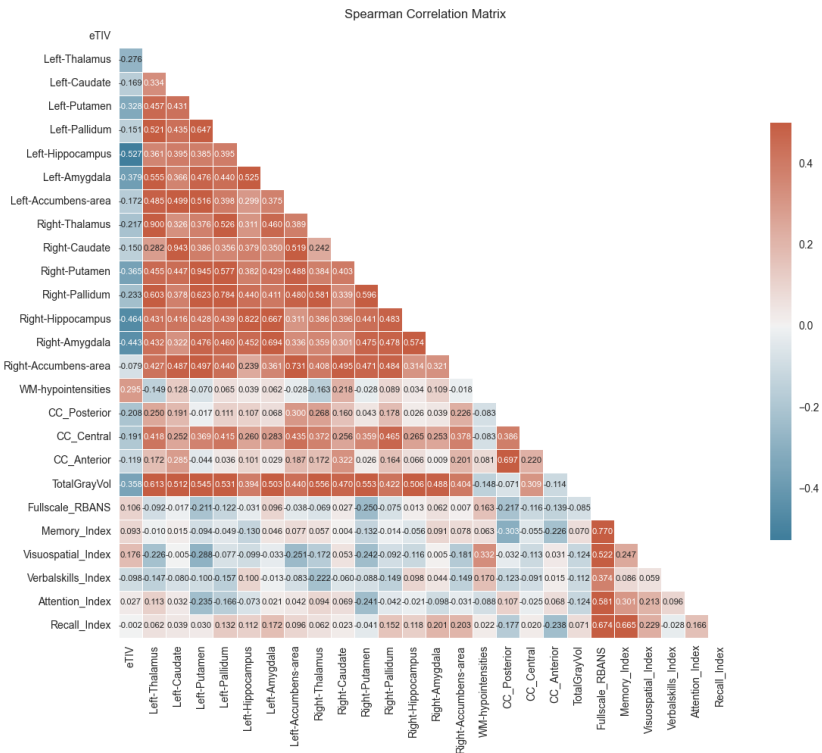
Figure 5. Pairwise correlations between the morphometric and cognitive variables

Prediction of IBS versus HC from morphometric and cognitive measures

The Extreme Gradient Boosting (xgboost) was also selected as the best model when cognitive features (the five indexes) were included as predictors together with the morphometric volume measures. An accuracy of 0.6500 in the training set improved to 0.6667 in the test set, and the confusion matrix shown in Figure 6 (a) indicates an improved generalization when cognitive features were included. The Figure shows that 93% of the IBS patients (14/15) were correctly classified (one misclassified man in the older age range). However, the specificity was lower, in that 78% in the HC group, all men, were misclassified as IBS patients.

Figure 6 illustrates how different brain measurements and cognitive abilities influence our model's predictions. Each row shows a different measurement, with the most influential features at the top. The dots represent individual participants, with red dots indicating higher values and blue dots indicating lower values for each measurement. The position of each dot shows whether that particular value pushes the model's prediction higher (towards the right) or lower (towards the left). The Right Hippocampus, shown at the top, has the strongest overall impact: when some people have high values (red dots), this strongly pushes predictions in one direction, while low values (blue dots) push predictions in the other direction. Verbal skills also shown important patterns, with a wide spread across different participants, suggesting that both high and low verbal skills can be important indicators, depending on the individual case. Among subcortical regions, Right Caudate and Right Putamen demonstrate particularly notable influences. These patterns reveal meaningful differences between our two groups in both brain structure and cognitive abilities. Particularly important are the variations we see in verbal abilities and in memory-

related brain regions like the hippocampus, which could inform how we approach patient care and communication strategies.
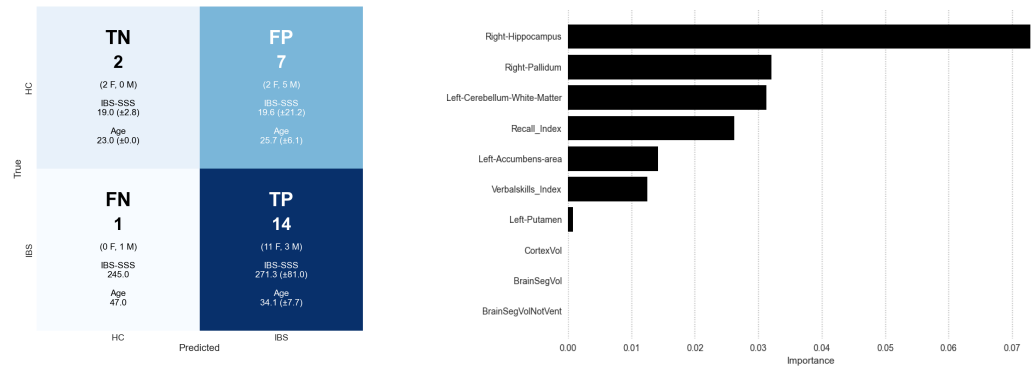

Figure 6. (a) Confusion matrix (XGBOOST) predicting IBS versus HC from brain morphometry and cognition. (b) Top 10 feature importance (permutation importance, 100 repeats) with Group (IBS vs HC) as the outcome variable and morphometric and cognitive features as predictors
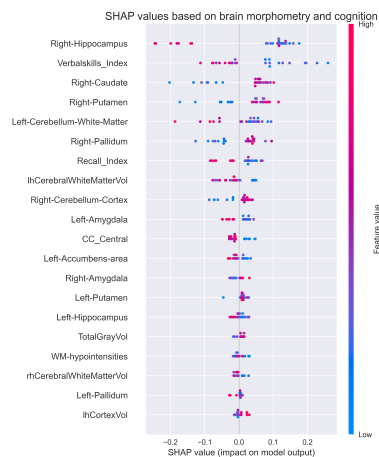

Figure 7. SHAP values with morhometry and cognition as predictors

Note:X-axis (SHAP values): The SHAP values indicate the impact each feature has on the model's output, which is the probability of classifying someone as IBS patient or HC.

Discussion

Our study yields two key methodological insights and one substantial findings regarding brain structure and function in IBS. First, we were unable to replicate the morphometric differences between the IBS and healthy control group reported by Skrobisz et al. [22], regardless of whether we used FreeSurfer version 6.0.1 or 7.4.1. Second, we observed substantial discrepancies in morphometric measurements between these software versions, highlighting the critical importance of considering methodological factors in neuroimaging research. Application of advanced multivariate and machine learning techniques to investigate brain-behavior relationships in IBS is another primary contribution. While morphometric features alone proved insufficient for reliable group discrimination, the integration of cognitive performance measures with brain morphometry substantially improved classification accuracy. Specifically, our analyses revealed that two cognitive domain indices, combined with volumetric measures of subcortical structures—particularly the hippocampus and basal ganglia—provided robust discrimination between IBS patients and healthy controls. The consistency of these findings across different approaches to feature

importance analyses strengthens their validity and suggests a fundamental relationship between brain structure, cognitive function, and IBS symptomatology. This observation aligns with views of IBS as a disorder involving complex interactions between central nervous system function and gastrointestinal symptoms, rather than purely peripheral manifestations.

Brain Structures involved in discriminating between IBS and HC

Our results showed that subcortical structures, particularly within the basal ganglia, played a key role in distinguishing IBS patients from healthy controls. While traditionally associated with motor control, the basal ganglia also critically influence reward processing, habit formation, and pain modulation - functions directly relevant to IBS symptomatology, and the impact on patients' experience of gastrointestinal symptoms. These findings align with recent results from a UK Biobank study [19], which also highlighted the importance of hippocampal and basal ganglia structures, including the Pallidum and Caudate, in IBS. Beyond the basal ganglia, several other subcortical structures relevant to IBS symptomatology emerged as discriminators. The nucleus accumbens, fundamental to reward processing and motivation, may mediate the emotional and motivational aspects of chronic pain in IBS. Dysfunction in this structure could explain the intensified emotional distress and pain sensitivity commonly reported by IBS patients [9]. Similarly, the amygdala appears significant, particularly given its connection to pain-modulation and emotion-processing networks, including the prefrontal cortex and insula. This aligns with previous research [36] demonstrating enhanced amygdala-insula connectivity in IBS patients. Although our results differ from Skrobisz et al.'s [22] findings regarding thalamic involvement, other studies have supported its role in IBS. Diffusion tensor imaging has revealed altered thalamic organization in IBS patients, with reduced fractional anisotropy and increased mean diffusivity [37]. These alterations suggest compromised structural integrity of thalamic circuits, potentially affecting pain processing and sensory integration. The involvement of corpus callosum should also be mentioned, as interhemospheric integration is crucial for visceral sensation processing, pain modulation [38] as well as in mental disorders [39]. Taken together, our fidnings support that integrated neural signatures are involved in predicting IBS [40].

Integration of Cognitive Performance and Brain Structure in IBS

The enhanced diagnostic accuracy by including cognitive measures strongly support that IBS should be understood as a disorder of the gut-brain interaction [14,41]. The brain's integral role in cognitive, emotional, and autonomic regulation suggests that these manifestations are fundamentally interconnected rather than merely coincidental. The prominent role of hippocampal volume was a principal finding. The fundamental role of Hippocampus in cognitive processing is well known [42], and was supported by the Recall index being identified as another feature with strong importance. The role of Verbal skills was more surprising. Although research has established connections between memory systems and language processing, particularly in semantic memory organization [43], a negliable correlation between the two indicies suggests that IBS affects multiple cognitive domains through independent mechanisms.

Our findings may also have implications for other somatic and psychiatric disorders, like Alzheimer's disease, Parkinson's disease, and major depression. The gut-brain axis are involved in all these diseases, which also are characterized by cognitive impairment. Recent research has identified potential pathways linking gut microbiota alterations to neurological function, particularly through inflammatory responses and tryptophan metabolism [44,45]. The emergence of the microbiota-gut-brain axis as a key framework [46] offers new perspectives on how peripheral inflammation might influence both brain structure and cognitive function in IBS. This integrated view suggests that cognitive assessment,

combined with brain morphometry, might provide valuable insights not only for IBS but for a broader spectrum of gut-brain disorders.

Brain-Gut Axis: Implications for Understanding and Treating IBS

Our findings should have important implications for clinical practice and treatment development. The observed relationship between brain structure, cognitive function, and IBS symptomatology suggests that effective interventions should target multiple domains simultaneously. Such a multifaceted approach recognizes IBS as a complex disorder requiring coordinated intervention across multiple domains.

Future research directions should expand upon these findings through multimodal investigation. Integration of functional neuroimaging, gut microbiome analysis, and broader clinical assessment [19] could provide a more comprehensive understanding of IBS pathophysiology. Particularly crucial will be longitudinal studies to determine the temporal relationship between brain changes and symptom development. Such studies would allow us to track the evolution of cognitive and structural alterations over time, identify early markers of disease progression, and evaluate the impact of various therapeutic interventions. This temporal perspective is essential for understanding whether observed brain changes represent cause or consequence of IBS symptoms.

This comprehensive approach to understanding IBS aligns with the emerging paradigm of precision medicine. By considering the full spectrum of biological, cognitive, and behavioral manifestations, we may better identify patient subgroups and develop more personalized treatment strategies. The integration of brain structure, cognitive function, and clinical symptoms represents a promising framework for advancing both our understanding and treatment of this complex disorder. Ultimately, this integrated perspective may lead to more effective, personalized interventions that address the full range of IBS manifestations.

Strengths and Limitations: Critical Evaluation and Future Directions

Although contributing through its multimodal analytical approach, several limitations warrant discussion. The primary limitation concerns sample size, which particularly constrained our ability to conduct robust sex/gender-based analyses. This limitation is especially noteworthy given the evidence for substantial sex/gender differences in IBS presentation, progression, and treatment response [47]. The importance of sex/gender considerations in IBS research has become increasingly apparent. Clinical presentations show clear sex-based patterns, with IBS-C predominating in women and IBS-D in men [48]. These differences reflect complex interactions between biological and environmental factors. Sex hormones, particularly estrogen and progesterone, influence both gastrointestinal function and pain processing in the central nervous system [49]. Recent research has revealed sex-based differences extending to gut microbiota composition [50] and sensory processing. Notably, Labus et al. [20] demonstrated enhanced sensory sensitivity in women with IBS, potentially related to sex-specific morphometric variations in brain structure.

An inability to fully account for IBS symptom severity in our analyses was abouther limitation. Recent work by Li et al. [19] has demonstrated that symptom severity correlates significantly with both cognitive performance and brain volumetric measures, particularly in regions associated with emotional processing and cognitive control. This finding suggests that future studies should incorporate detailed severity measures to better understand the relationship between symptom intensity and brain-behavior patterns.

The present study's methodological strengths lie in its comprehensive multivariate approach to analyzing brain-behavior relationships. This approach better captures the complex interactions between multiple brain regions and cognitive measures, providing a more nuanced understanding than traditional univariate analyses. However, we acknowledge important limitations. While our sample exceeds that of many comparable studies, multi-

variate analyses and machine learning approaches typically benefit from larger datasets. To address this limitation, we implemented robust cross-validation procedures, including 10-fold validation and hold-out test sets, thereby reducing the risk of overfitting and enhancing the generalizability of our findings. Moreover, the results point to several important directions for future research. First, larger-scale studies are needed to validate and extend our multivariate findings. Such studies should maintain rigorous methodological standards while increasing statistical power. Second, standardization of neuroimaging analysis protocols, including careful documentation of software versions and processing parameters, is crucial for reproducibility. Third, the field would benefit from systematic investigation of how different analysis approaches might influence morphometric findings in IBS research. Overall, future studies should consider implementing standardized protocols for both imaging and cognitive assessment, facilitating meta-analyses and enabling more direct comparisons across studies. This standardization, combined with transparent reporting of methodological details, would strengthen the field's ability to build cumulative knowledge about brain-gut interactions in IBS. Longitudinal studies represent a particularly important future direction. Such studies could address crucial questions about the temporal dynamics of brain-gut interactions in IBS, including whether observed structural and cognitive changes precede or follow symptom development. Longitudinal data would also enable better prediction of disease trajectories and treatment responses, potentially informing personalized interventions such as dietary modifications (e.g., Low FODMAP diet) or targeted cognitive interventions. The combination of longitudinal design with multimodal assessment (including brain structure, cognitive function, and clinical symptoms) could provide unprecedented insights into the development and progression of IBS.

Conclusions and Future Directions

The present study advances our understanding of brain-gut interactions in IBS through several key contributions. First, our comprehensive multivariate analyses reveal the inherent complexity of IBS pathophysiology, demonstrating that single-modality approaches may be insufficient for characterizing this multifaceted disorder. While we did not replicate previously reported volumetric differences in thalamic structure, our machine learning analyses uncovered more subtle and complex patterns of brain-behavior relationships. Particularly noteworthy was the finding that morphometric features gain discriminative power when integrated with cognitive measures, especially in subcortical regions including the hippocampus and basal ganglia. These results strongly support a systems-level conceptualization of IBS, where the condition emerges from complex interactions between neural structure, cognitive function, and gastrointestinal symptoms. This perspective suggests that effective characterization and treatment of IBS requires consideration of multiple biological and cognitive markers rather than focusing on isolated symptoms or structures. The successful integration of structural and functional measures in our analyses points toward more sophisticated approaches for both diagnosis and treatment planning.

Moving forward, several research priorities emerge from our findings. Large-scale validation studies are needed to confirm the reliability and generalizability of our brain-cognition relationships across diverse patient populations. Such studies should incorporate standardized protocols for both imaging and cognitive assessment to facilitate cross-study comparisons. Longitudinal investigations are particularly crucial for understanding how these markers evolve over time and relate to treatment response. Additionally, future research should explore how individual differences in brain structure and cognitive function might predict treatment outcomes, potentially enabling more personalized therapeutic approaches. ´Ultimately, our findings suggest that advancing IBS treatment may require a fundamental shift toward integrated, multimodal assessment approaches that capture both structural and functional aspects of brain-gut interactions. This more comprehensive understanding of IBS pathophysiology could lead to more effective, personalized interventions that address the full spectrum of patient symptoms and experiences.

References

1. Black, C.J.; Ford, A.C. Global burden of irritable bowel syndrome: trends, predictions and risk factors. *Nature Reviews Gastroenterology & hepatology* **2020**, *17*, 473–486. https://doi.org/10.1038/s41575-020-0286-8.

2. Lovell, R.M.; Ford, A.C. Global prevalence of and risk factors for irritable bowel syndrome: a meta-analysis. *Clinical Gastroenterology and Hepatology* **2012**, *10*, 712–721. https://doi.org/10.1016/j.cgh.2012.02.029.

3. Bonetto, S.; Fagoonee, S.; Battaglia, E.; Grassini, M.; Saracco, G.M.; Pellicano, R. Recent advances in the treatment of irritable bowel syndrome. *Polish Archives of Internal Medicine* **2021**, *131*, 709–715. https://doi.org/10.20452/pamw.16067.

4. Drossman, D.A.; Tack, J. Rome Foundation clinical diagnostic criteria for disorders of gut-brain interaction. *Gastroenterology* **2022**, *162*, 675–679. https://doi.org/10.1053/j.gastro.2021.11.019.

5. Heitkemper, M.M.; Cain, K.C.; Jarrett, M.E.; Burr, R.L.; Hertig, V.; Bond, E.F. Symptoms across the menstrual cycle in women with irritable bowel syndrome. *Official Journal of the American College of Gastroenterology | ACG* **2003**, *98*, 420–430. https://doi.org/10.1111/j.1572-0241.2003.07233.x.

6. Meleine, M.; Matricon, J. Gender-related differences in irritable bowel syndrome: potential mechanisms of sex hormones. *World Journal of Gastroenterology: WJG* **2014**, *20*, 6725. https://doi.org/10.3748/wjg.v20.i22.6725.

7. Kim, Y.S.; Kim, N. Sex-gender differences in irritable bowel syndrome. *Journal of Neurogastroenterology and Motility* **2018**, *24*, 544.

8. Toner, B.B.; Akman, D. Gender role and irritable bowel syndrome: literature review and hypothesis. *Official journal of the American College of Gastroenterology | ACG* **2000**, *95*, 11–16. https://doi.org/10.1111/j.1572-0241.2000.01698.x.

9. Lundervold, A.J.; Billing, J.E.; Berentsen, B.; Lied, G.A.; Steinsvik, E.K.; Hausken, T.; Lundervold, A. Decoding IBS: a machine learning approach to psychological distress and gut-brain interaction. *BMC Gastroenterology* **2024**, *24*, 267. https://doi.org/10.1186/s12876-024-03355-z.

10. Shiha, M.G.; Aziz, I. Physical and psychological comorbidities associated with irritable bowel syndrome. *Alimentary Pharmacology & Therapeutics* **2021**, *54*, S12–S23. https://doi.org/10.1111/apt.16589.

11. Lam, N.C.Y.; Yeung, H.Y.; Li, W.K.; Lo, H.Y.; Yuen, C.F.; Chang, R.C.C.; Ho, Y.S. Cognitive impairment in irritable bowel syndrome (IBS): a systematic review. *Brain Research* **2019**, *1719*, 274–284. https://doi.org/https://doi.org/10.1016/j.brainres.2019.05.036.

12. Wong, K.M.F.; Mak, A.D.P.; Yuen, S.Y.; Leung, O.N.W.; Ma, D.Y.; Chan, Y.; Cheong, P.K.; Lui, R.; Wong, S.H.; Wu, J.C.Y. Nature and specificity of altered cognitive functioning in IBS. *Neurogastroenterology & Motility* **2019**, *31*, e13696. https://doi.org/10.1111/nmo.13696.

13. Billing, J.; Berentsen, B.; Lundervold, A.; Hillestad, E.M.; Lied, G.A.; Hausken, T.; Lundervold, A.J. Cognitive function in patients with irritable bowel syndrome: impairment is common and only weakly correlated with depression/anxiety and severity of gastrointestinal symptoms. *Scandinavian Journal of Gastroenterology* **2023**, pp. 1–9. https://doi.org/10.1080/00365521.2023.2256916.

14. Mayer, E.A.; Nance, K.; Chen, S. The Gut-Brain Axis. *Annual Review of Medicine* **2022**, *73*, 439–453. https://doi.org/10.1146/annurev-med-042320-014032.

15. Coss-Adame, E.; Rao, S.S. Brain and gut interactions in irritable bowel syndrome: new paradigms and new understandings. *Current Gastroenterology Reports* **2014**, *16*, 1–8. https://doi.org/10.1007/s11894-014-0379-z.

16. Lezak, M.D. *Neuropsychological assessment*; Oxford University Press, USA, 2004.

17. Park, H.J.; Friston, K. Structural and functional brain networks: from connections to cognition. *Science* **2013**, *342*, 1238411. https://doi.org/10.1126/science.1238411.

18. Mayer, E.A.; Labus, J.S.; Tillisch, K.; Cole, S.W.; Baldi, P. Towards a systems view of IBS. *Nature Reviews Gastroenterology & Hepatology* **2015**, *12*, 592–605. https://doi.org/10.1038/nrgastro.2015.121.

19. Li, Z.; Ma, Q.; Deng, Y.; Rolls, E.T.; Shen, C.; Li, Y.; Zhang, W.; Xiang, S.; Langley, C.; Sahakian, B.J.; et al. Irritable Bowel Syndrome Is Associated With Brain Health by Neuroimaging, Behavioral, Biochemical, and Genetic Analyses. *Biological Psychiatry* **2024**, *95*, 1122–1132. https://doi.org/10.1016/j.biopsych.2023.12.024.

20. Labus, J.S.; Wang, C.; Mayer, E.A.; Gupta, A.; Oughourlian, T.; Kilpatrick, L.; Tillisch, K.; Chang, L.; Naliboff, B.; Ellingson, B.M. Sex-specific brain microstructural reorganization in irritable bowel syndrome. *Pain* **2023**, *164*, 292–304. https://doi.org/10.1097/j.pain.0000000000002699.

21. Nan, J.; Yang, W.; Meng, P.; Huang, W.; Zheng, Q.; Xia, Y.; Liu, F. Changes of the postcentral cortex in irritable bowel syndrome patients. *Brain Imaging and Behavior* **2020**, *14*, 1566–1576.

22. Skrobisz, K.; Piotrowicz, G.; Rudnik, A.; Naumczyk, P.; Sabisz, A.; Markiet, K.; Szurowska, E. Evaluation of subcortical structure volumes in patients with non-specific digestive diseases. *Diagnostics* **2022**, *12*, 2199. https://doi.org/10.3390/diagnostics12092199.

23. Berentsen, B.; Nagaraja, B.H.; Teige, E.P.; Lied, G.A.; Lundervold, A.J.; Lundervold, K.; Steinsvik, E.K.; Hillestad, E.R.; Valeur, J.; Brønstad, I.; et al. Study protocol of the Bergen brain-gut-microbiota-axis study: A prospective case-report characterization and dietary intervention study to evaluate the effects of microbiota alterations on cognition and anatomical and functional brain connectivity in patients with irritable bowel syndrome. *Medicine* **2020**, *99*, e21950. https://doi.org/doi:10.1097/MD.0000000000021950.

24. Francis, C.Y.; Morris, J.; Whorwell, P.J. The irritable bowel severity scoring system: a simple method of monitoring irritable bowel syndrome and its progress. *Alimentary pharmacology & therapeutics* **1997**, *11*, 395–402. https://doi.org/10.1046/j.1365-2036.1997.142318000.x.

25. Randolph, C. *Repeatable battery for the assessment of neuropsychological status. Norwegian manual*; NL:Pearson, 2013.

26. Fischl, B. FreeSurfer. *Neuroimage* **2012**, *62*, 774–781. https://doi.org/10.1016/j.neuroimage.2012.01.021.

27. Klauschen, F.; Goldman, A.; Barra, V.; Meyer-Lindenberg, A.; Lundervold, A. Evaluation of automated brain MR image segmentation and volumetry methods. *Human Brain MApping* **2009**, *30*, 1310–1327. https://doi.org/https://doi.org/10.1002/hbm.20599.

28. Jovicich, J.; Czanner, S.; Han, X.; Salat, D.; van der Kouwe, A.; Quinn, B.; Pacheco, J.; Albert, M.; Killiany, R.; Blacker, D.; et al. MRI-derived measurements of human subcortical, ventricular and intracranial brain volumes: reliability effects of scan sessions, acquisition sequences, data analyses, scanner upgrade, scanner vendors and field strengths. *Neuroimage* **2009**, *46*, 177–192. https://doi.org/https://doi.org/10.1016/j.neuroimage.2009.02.010.

29. Gronenschild, E.H.; Habets, P.; Jacobs, H.I.; Mengelers, R.; Rozendaal, N.; Van Os, J.; Marcelis, M. The effects of FreeSurfer version, workstation type, and Macintosh operating system version on anatomical volume and cortical thickness measurements. *PloS One* **2012**, *7*, e38234. https://doi.org/https://doi.org/10.1371/journal.pone.0038234.

30. Glatard, T.; Lewis, L.B.; Ferreira da Silva, R.; Adalat, R.; Beck, N.; Lepage, C.; Rioux, P.; Rousseau, M.E.; Sherif, T.; Deelman, E.; et al. Reproducibility of neuroimaging analyses across operating systems. *Frontiers in Neuroinformatics* **2015**, *9*, 12. https://doi.org/https://doi.org/10.3389/fninf.2015.00012.

31. Knussmann, G.N.; Anderson, J.S.; Prigge, M.B.; Dean III, D.C.; Lange, N.; Bigler, E.D.; Alexander, A.L.; Lainhart, J.E.; Zielinski, B.A.; King, J.B. Test-retest reliability of FreeSurfer-derived volume, area and cortical thickness from MPRAGE and MP2RAGE brain MRI images. *Neuroimage: Reports* **2022**, *2*, 100086. https://doi.org/10.1016/j.ynirp.2022.100086.

32. Debiasi, G.; Mazzonetto, I.; Bertoldo, A. The effect of processing pipelines, input images and age on automatic cortical morphology estimates. *Computer Methods and Programs in Biomedicine* **2023**, *242*, 107825. https://doi.org/https://doi.org/10.1016/j.cmpb.2023.107825.

33. Kirk, R.E. Practical significance: A concept whose time has come. *Educational and psychological measurement* **1996**, *56*, 746–759.

34. Xiang, S.; Nie, F.; Zhang, C. Learning a Mahalanobis distance metric for data clustering and classification. *Pattern Recognition* **2008**, *41*, 3600–3612.

35. Lundberg, S.M.; Erion, G.; Chen, H.; DeGrave, A.; Prutkin, J.M.; Nair, B.; Katz, R.; Himmelfarb, J.; Bansal, N.; Lee, S.I. From local explanations to global understanding with explainable AI for trees. *Nature machine intelligence* **2020**, *2*, 56–67. https://doi.org/10.1038/s42256-019-0138-9.

36. Qi, R.; Liu, C.; Ke, J.; Xu, Q.; Ye, Y.; Jia, L.; Wang, F.; Zhang, L.; Lu, G. Abnormal amygdala resting-state functional connectivity in irritable bowel syndrome. *American Journal of Neuroradiology* **2016**, *37*, 1139–1145.

37. Ellingson, B.M.; Mayer, E.; Harris, R.J.; Ashe-McNally, C.; Naliboff, B.D.; Labus, J.S.; Tillisch, K. Diffusion tensor imaging detects microstructural reorganization in the brain associated with chronic irritable bowel syndrome. *PAIN®* **2013**, *154*, 1528–1541. https://doi.org/10.1016/j.pain.2013.04.010.

38. Ito, A.; Yang, S.; Shinto, E.; Shinto, A.; Toyofuku, A.; Kurata, J. Interhemispheric and Corticothalamic White-Matter Dysfunction Underlies Affective Morbidity and Impaired Pain Modulation in Chronic Pain. *Anesthesia & Analgesia* **2022**, pp. 10–1213. https://doi.org/10.1213/ANE.0000000000006992.

39. Piras, F.; Vecchio, D.; Kurth, F.; Piras, F.; Banaj, N.; Ciullo, V.; Luders, E.; Spalletta, G. Corpus callosum morphology in major mental disorders: a magnetic resonance imaging study. *Brain Communications* **2021**, *3*, fcab100. https://doi.org/10.1093/braincomms/fcab100.
40. Bhatt, R.R.; Gupta, A.; Labus, J.S.; Liu, C.; Vora, P.P.; Stains, J.; Naliboff, B.D.; Mayer, E.A. A neuropsychosocial signature predicts longitudinal symptom changes in women with irritable bowel syndrome. *Molecular Psychiatry* **2022**, *27*, 1774–1791. https://doi.org/0.1038/s41380-021-01375-9.
41. Zhao, M.; Hao, Z.; Li, M.; Xi, H.; Hu, S.; Wen, J.; Gao, Y.; Antwi, C.O.; Jia, X.; Yu, Y.; et al. Functional changes of default mode network and structural alterations of gray matter in patients with irritable bowel syndrome: a meta-analysis of whole-brain studies. *Frontiers in Neuroscience* **2023**, *17*, 1236069. https://doi.org/10.3389/fnins.2023.1236069.
42. Lisman, J.; Buzsáki, G.; Eichenbaum, H.; Nadel, L.; Ranganath, C.; Redish, A.D. Viewpoints: how the hippocampus contributes to memory, navigation and cognition. *Nature Neuroscience* **2017**, *20*, 1434–1447.
43. Burgess, N.; Maguire, E.A.; O'Keefe, J. The human hippocampus and spatial and episodic memory. *Neuron* **2002**, *35*, 625–641. https://doi.org/10.1016/s0896-6273(02)00830-9.
44. Sibelli, A.; Chalder, T.; Everitt, H.; Workman, P.; Windgassen, S.; Moss-Morris, R. A systematic review with meta-analysis of the role of anxiety and depression in irritable bowel syndrome onset. *Psychological Medicine* **2016**, *46*, 3065–3080. https://doi.org/10.1017/S0033291716001987.
45. Carloni, S.; Rescigno, M. The gut-brain vascular axis in neuroinflammation. In Proceedings of the Seminars in immunology. Elsevier, 2023, Vol. 69, p. 101802. https://doi.org/10.1016/j.smim.2023.101802.
46. Ishioh, M.; Nozu, T.; Okumura, T. Brain Neuropeptides, Neuroinflammation, and Irritable Bowel Syndrome. *Digestion* **2024**, *105*, 34–39. https://doi.org/10.1159/000533275.
47. van Kessel, L.; Teunissen, D.; Lagro-Janssen, T. Sex-gender differences in the effectiveness of treatment of irritable bowel syndrome: A systematic review. *International Journal of General Medicine*, pp. 867–884. https://doi.org/10.2147/IJGM.S291964.
48. Lee, O.Y.; Mayer, E.A.; Schmulson, M.; Chang, L.; Naliboff, B. Gender-related differences in IBS symptoms. *Official journal of the American College of Gastroenterology | ACG* **2001**, *96*, 2184–2193.
49. Chang, L.; Heitkemper, M.M. Gender differences in irritable bowel syndrome. *Gastroenterology* **2002**, *123*, 1686–1701. https://doi.org/10.1053/gast.2002.36603.
50. Vemuri, R.; Sylvia, K.E.; Klein, S.L.; Forster, S.C.; Plebanski, M.; Eri, R.; Flanagan, K.L. The microgenderome revealed: sex differences in bidirectional interactions between the microbiota, hormones, immunity and disease susceptibility. In Proceedings of the Seminars in immunopathology. Springer, 2019, Vol. 41, pp. 265–275.

Data Availability Statement: We encourage all authors of articles published in MDPI journals to share their research data. In this section, please provide details regarding where data supporting reported results can be found, including links to publicly archived datasets analyzed or generated during the study. Where no new data were created, or where data is unavailable due to privacy or ethical restrictions, a statement is still required. Suggested Data Availability Statements are available in section "MDPI Research Data Policies" at https://www.mdpi.com/ethics.

Abbreviations

The following abbreviations are used in the manuscript:

AUC	Area Under Curve
CM	Confusion matrix
Cohen's d	effect size
Cliff's delta	effect size
DGBI	Disorders of the gut-brain interaction
FS	Freesurfer
GI	Gastrointestinal
GitHub	Meeting platform for collaboration
HC	Healthy Control
IBS	Irritable bowel syndrome
IBS-SSS	IBS Severity Scoring System
IQR	Inter Quartice Range
ML	Machine-learning
MRI	Magnetic Resonance Imaging
RBANS	Repeatable Battery for the Assessment of Neuropsychological Status
RF	Random Forest
ROC	Operating Characteristic
SHAP	SHapley Additive exPlanations
SD	Standard deviation
SHAP	SHapley Additive exPlanations
XGBoost	eXtreme Gradient Boosting

Appendix A

Appendix A.1

Table A1. FreeSurfer segmented brain regions (`aseg`) with short descriptions of functional anatomy

Region	Description
eTIV	Estimated Total Intracranial Volume
Left-Cerebellum-White-Matter	White matter in the left cerebellum
Left-Cerebellum-Cortex	Gray matter (cortex) in the left cerebellum
Left-Thalamus	Left thalamus. *Thalamus* is a relay center for sensory and motor signals. In IBS, thalamic activity will contribute to pain perception and visceral hypersensitivity
Left-Caudate	Left caudate nucleus. *Nucleus caudatus* is involved in motor and motility control and learning
Left-Putamen	Left putamen. *Putamen* is part of the basal ganglia involved in motor control and may contribute to habitual responses to gastrointestinal discomfort
Left-Pallidum	Left globus pallidus. *Globus pallidus* is involved in regulating voluntary movement and gut motility patterns
Left-Hippocampus	Left hippocampus. *Hippocampus* is crucial for memory formation and spatial navigation, and in IBS, involved in contextual fear learning related to gastrointestinal symptoms
Left-Amygdala	Left amygdala. *Amygdala* is involved in processing emotions, fear, and anxiety
Left-Accumbens-area	Left nucleus accumbens. *Nucleus accumbens* is involved in reward and motivation, stress responsivity, and pain modulation
CSF	Cerebrospinal Fluid
Right-Cerebellum-White-Matter	White matter in the right cerebellum
Right-Cerebellum-Cortex	Gray matter (cortex) in the right cerebellum
Right-Thalamus	Right thalamus
Right-Caudate	Right caudate nucleus
Right-Putamen	Right putamen
Right-Pallidum	Right globus pallidus
Right-Hippocampus	Right hippocampus
Right-Amygdala	Right amygdala
Right-Accumbens-area	Right nucleus accumbens
WM-hypointensities	White matter hypointensities (dark on T1-w sequences), can be associated with small vessel disease, demyelination, inflammation, fluid accumulation
CC_Posterior	Posterior part of the corpus callosum
CC_Mid_Posterior	Mid-posterior part of the corpus callosum
CC_Central	Central part of the corpus callosum
CC_Mid_Anterior	Mid-anterior part of the corpus callosum
CC_Anterior	Anterior part of the corpus callosum
BrainSegVol	Total volume of brain segmentation
BrainSegVolNotVent	Brain segmentation volume without ventricles
lhCortexVol	Volume of the left hemisphere cortex
rhCortexVol	Volume of the right hemisphere cortex
CortexVol	Total cortical volume (left + right)
lhCerebralWhiteMatterVol	Volume of left hemisphere cerebral white matter
rhCerebralWhiteMatterVol	Volume of right hemisphere cerebral white matter
CerebralWhiteMatterVol	Total cerebral white matter volume (left + right)
SubCortGrayVol	Volume of subcortical gray matter
TotalGrayVol	Total gray matter volume

864

865

Table A2. Comparison of Brain Region eTIV-normalized Volumes (mean $\pm$ std) in HC and IBS Patients (FS 7.4.1)

eTIV HC: 1492943.664536 $\pm$ 171477.74473 [mm^3]   eTIV IBS: 1464197.188161 $\pm$ 143328.070214 [mm^3]

Feature	HC	IBS
Left-Cerebellum-White-Matter	0.010888 $\pm$ 0.001076	0.010688 $\pm$ 0.001044
Left-Cerebellum-Cortex	0.037438 $\pm$ 0.003633	0.037232 $\pm$ 0.003575
Left-Thalamus	0.005385 $\pm$ 0.000517	0.005262 $\pm$ 0.000473
Left-Caudate	0.002506 $\pm$ 0.000313	0.002474 $\pm$ 0.000315
Left-Putamen	0.003702 $\pm$ 0.000418	0.003621 $\pm$ 0.000369
Left-Pallidum	0.001415 $\pm$ 0.000156	0.001373 $\pm$ 0.000098
Left-Hippocampus	0.002970 $\pm$ 0.000273	0.002925 $\pm$ 0.000244
Left-Amygdala	0.001253 $\pm$ 0.000138	0.001203 $\pm$ 0.000111
Left-Accumbens-area	0.000440 $\pm$ 0.000072	0.000429 $\pm$ 0.000070
CSF	0.000712 $\pm$ 0.000127	0.000742 $\pm$ 0.000130
Right-Cerebellum-White-Matter	0.010218 $\pm$ 0.001008	0.010231 $\pm$ 0.000955
Right-Cerebellum-Cortex	0.038471 $\pm$ 0.003722	0.038176 $\pm$ 0.003654
Right-Thalamus	0.005475 $\pm$ 0.000474	0.005341 $\pm$ 0.000456
Right-Caudate	0.002608 $\pm$ 0.000310	0.002577 $\pm$ 0.000303
Right-Putamen	0.003788 $\pm$ 0.000418	0.003766 $\pm$ 0.000375
Right-Pallidum	0.001350 $\pm$ 0.000156	0.001330 $\pm$ 0.000120
Right-Hippocampus	0.003102 $\pm$ 0.000245	0.003034 $\pm$ 0.000241
Right-Amygdala	0.001332 $\pm$ 0.000115	0.001323 $\pm$ 0.000115
Right-Accumbens-area	0.000503 $\pm$ 0.000065	0.000507 $\pm$ 0.000063
WM-hypointensities	0.000757 $\pm$ 0.000644	0.000607 $\pm$ 0.000274
CC_Posterior	0.000632 $\pm$ 0.000097	0.000669 $\pm$ 0.000112
CC_Mid_Posterior	0.000350 $\pm$ 0.000066	0.000375 $\pm$ 0.000075
CC_Central	0.000364 $\pm$ 0.000082	0.000363 $\pm$ 0.000091
CC_Mid_Anterior	0.000361 $\pm$ 0.000071	0.000379 $\pm$ 0.000101
CC_Anterior	0.000587 $\pm$ 0.000096	0.000620 $\pm$ 0.000093
BrainSegVol	0.798892 $\pm$ 0.038555	0.790867 $\pm$ 0.029736
BrainSegVolNotVent	0.785834 $\pm$ 0.038695	0.776074 $\pm$ 0.031471
lhCortexVol	0.170575 $\pm$ 0.010496	0.168994 $\pm$ 0.010110
rhCortexVol	0.170608 $\pm$ 0.010675	0.168900 $\pm$ 0.009646
CortexVol	0.341183 $\pm$ 0.021084	0.337894 $\pm$ 0.019676
lhCerebralWhiteMatterVol	0.153875 $\pm$ 0.009612	0.151551 $\pm$ 0.009309
rhCerebralWhiteMatterVol	0.152915 $\pm$ 0.009898	0.150025 $\pm$ 0.009752
CerebralWhiteMatterVol	0.306790 $\pm$ 0.019437	0.301576 $\pm$ 0.018991
SubCortGrayVol	0.042919 $\pm$ 0.003186	0.042213 $\pm$ 0.002739
TotalGrayVol	0.459994 $\pm$ 0.028590	0.455681 $\pm$ 0.025742

Table A3. Comparison of IBS and HC aseg volumes in FS6

Volume	Normality IBS pval	Normality HC pval	Comparison pval	Bonferroni pval	Comment
Left-Lateral-Ventricle	0.000000	0.012262	0.218568	1	Mann-Whitney U
Right-Lateral-Ventricle	0.000000	0.003318	0.175604	1	Mann-Whitney U
Left-Inf-Lat-Vent	0.027017	0.065782	0.306041	1	Mann-Whitney U
Right-Inf-Lat-Vent	0.000125	0.213863	1.000000	1	Mann-Whitney U
Left-Cerebellum-White-Matter	0.868712	0.985446	0.949833	1	
Right-Cerebellum-White-Matter	0.603141	0.706852	0.976594	1	
Left-Cerebellum-Cortex	0.887605	0.482798	0.653898	1	
Right-Cerebellum-Cortex	0.702170	0.592983	0.758101	1	
Left-Thalamus	0.020665	0.155399	0.301181	1	Mann-Whitney U
Right-Thalamus	0.224706	0.851854	0.610332	1	
Left-Caudate	0.193917	0.095106	0.982940	1	
Right-Caudate	0.475606	0.154798	0.986886	1	
Left-Putamen	0.593210	0.644070	0.673866	1	
Right-Putamen	0.359791	0.386205	0.834282	1	
Left-Pallidum	0.173697	0.989181	0.344000	1	
Right-Pallidum	0.595734	0.947931	0.424336	1	
Left-Hippocampus	0.287700	0.860954	0.786233	1	
Right-Hippocampus	0.759612	0.516918	0.592959	1	
Left-Amygdala	0.912786	0.830186	0.545057	1	
Right-Amygdala	0.593246	0.433174	0.547507	1	
Left-Accumbens	0.488757	0.065034	0.682336	1	
Right-Accumbens	0.509006	0.415282	0.912534	1	
Left-VentralDC	0.002720	0.588560	0.950536	1	Mann-Whitney U
Right-VentralDC	0.005949	0.284419	0.917653	1	Mann-Whitney U
Left-vessel	0.000401	0.094311	0.508154	1	Mann-Whitney U
Right-vessel	0.000000	0.005442	0.521457	1	Mann-Whitney U
Left-choroid-plexus	0.016097	0.219801	0.501560	1	Mann-Whitney U
Right-choroid-plexus	0.019767	0.029370	0.514815	1	Mann-Whitney U
3rd-Ventricle	0.000000	0.000362	0.893080	1	Mann-Whitney U
4th-Ventricle	0.001158	0.024413	0.634362	1	Mann-Whitney U
Brain-Stem	0.137448	0.360370	0.768517	1	
CSF	0.003523	0.008289	0.402333	1	Mann-Whitney U
WM-hypointensities	0.000008	0.000006	0.029916	1	Mann-Whitney U
Optic-Chiasm	0.123529	0.551434	0.013754	0.550162	
$CC_{posterior}$	0.959319	0.933417	0.041734	1	
$CC_{Mid_{posterior}}$	0.922474	0.176344	0.054800	1	
$CC_{central}$	0.000569	0.001136	0.764305	1	Mann-Whitney U
$CC_{Mid_{Anterior}}$	0.011289	0.096757	0.341507	1	Mann-Whitney U
$CC_{Anterior}$	0.826186	0.873424	0.238267	1	
eTIV	0.247179	0.251004	0.226989	1	

Table A4. Comparison of IBS and HC aseg volumes in FS7

Volume	Normality IBS pval	Normality HC pval	Comparison pval	Comparison pval Bonferroni	Comment
Left-Lateral-Ventricle	0.000000	0.009300	0.246875	1	Mann-Whitney U
Right-Lateral-Ventricle	0.000000	0.002694	0.207178	1	Mann-Whitney U
Left-Inf-Lat-Vent	0.080131	0.088521	0.856348	1	
Right-Inf-Lat-Vent	0.000133	0.260428	0.868610	1	Mann-Whitney U
Left-Cerebellum-White-Matter	0.004976	0.851036	0.958772	1	Mann-Whitney U
Right-Cerebellum-White-Matter	0.003845	0.682588	0.893080	1	Mann-Whitney U
Left-Cerebellum-Cortex	0.283041	0.162940	0.990895	1	
Right-Cerebellum-Cortex	0.186949	0.236715	0.970661	1	
Left-Thalamus	0.629663	0.989272	0.302305	1	
Right-Thalamus	0.757557	0.708280	0.188223	1	
Left-Caudate	0.297307	0.043358	0.748582	1	Mann-Whitney U
Right-Caudate	0.600437	0.023034	0.950536	1	Mann-Whitney U
Left-Putamen	0.759159	0.915929	0.438293	1	
Right-Putamen	0.333399	0.636413	0.804978	1	
Left-Pallidum	0.078100	0.919559	0.447175	1	
Right-Pallidum	0.430847	0.529711	0.630579	1	
Left-Hippocampus	0.753669	0.930149	0.589836	1	
Right-Hippocampus	0.630679	0.282365	0.251339	1	
Left-Amygdala	0.201884	0.352310	0.197443	1	
Right-Amygdala	0.182933	0.074914	0.720138	1	
Left-Accumbens	0.462705	0.666103	0.092410	1	
Right-Accumbens	0.728234	0.867678	0.921978	1	
Left-VentralDC	0.113865	0.322760	0.347871	1	
Right-VentralDC	0.084639	0.458216	0.748571	1	
Left-vessel	0.000674	0.145765	0.511390	1	Mann-Whitney U
Right-vessel	0.000001	0.295858	0.840137	1	Mann-Whitney U
Left-choroid-plexus	0.007234	0.070964	0.844264	1	Mann-Whitney U
Right-choroid-plexus	0.004609	0.005567	0.535033	1	Mann-Whitney U
3rd-Ventricle	0.000000	0.000188	0.917653	1	Mann-Whitney U
4th-Ventricle	0.003214	0.013104	0.521510	1	Mann-Whitney U
Brain-Stem	0.126983	0.279373	0.690067	1	
CSF	0.001306	0.265190	0.346781	1	Mann-Whitney U
WM-hypointensities	0.000001	0.000000	0.038658	1	Mann-Whitney U
Optic-Chiasm	0.036428	0.718661	0.336286	1	Mann-Whitney U
$CC_{posterior}$	0.945735	0.972734	0.100319	1	
$CC_{Mid_{posterior}}$	0.744740	0.381193	0.104056	1	
$CC_{central}$	0.032609	0.047760	0.975256	1	Mann-Whitney U
$CC_{Mid_{Anterior}}$	0.018030	0.412306	0.709740	1	Mann-Whitney U
$CC_{Anterior}$	0.923836	0.626622	0.115223	1	
eTIV	0.097863	0.208487	0.403217	1	

Table A5. Comparison of FS6 and FS7 aseg volumes in IBS group

Volume	Normality differences pval	Comparison pval	Comparison pval Bonferroni	Comment
Left-Lateral-Ventricle	0.000000	0.000087	0.003472	Wilcoxon
Right-Lateral-Ventricle	0.000000	0.000000	0.000001	Wilcoxon
Left-Inf-Lat-Vent	0.375408	0.000009	0.000378	
Right-Inf-Lat-Vent	0.158059	0.818370	1	
Left-Cerebellum-White-Matter	0.005076	0.447088	1	Wilcoxon
Right-Cerebellum-White-Matter	0.000007	0.128844	1	Wilcoxon
Left-Cerebellum-Cortex	0.000002	0.000000	0.000007	Wilcoxon
Right-Cerebellum-Cortex	0.000033	0.000001	0.000050	Wilcoxon
Left-Thalamus	0.006281	0.107526	1	Wilcoxon
Right-Thalamus	0.100475	0.599563	1	
Left-Caudate	0.000309	0.000139	0.005566	Wilcoxon
Right-Caudate	0.000010	0.000091	0.003643	Wilcoxon
Left-Putamen	0.000000	0.000035	0.001418	Wilcoxon
Right-Putamen	0.000239	0.012341	0.493641	Wilcoxon
Left-Pallidum	0.000363	0.011630	0.465197	Wilcoxon
Right-Pallidum	0.057175	0.565184	1	
Left-Hippocampus	0.042432	0.601096	1	Wilcoxon
Right-Hippocampus	0.000350	0.560480	1	Wilcoxon
Left-Amygdala	0.253044	0.145429	1	
Right-Amygdala	0.652820	0.180243	1	
Left-Accumbens	0.028440	0.000100	0.004007	Wilcoxon
Right-Accumbens	0.397144	0.072430	1	
Left-VentralDC	0.042749	0.000000	0.000001	Wilcoxon
Right-VentralDC	0.073781	0.008492	0.339688	
Left-vessel	0.000317	0.949374	1	Wilcoxon
Right-vessel	0.028412	0.000200	0.007993	Wilcoxon
Left-choroid-plexus	0.545034	0.033533	1	
Right-choroid-plexus	0.962062	0.538539	1	
3rd-Ventricle	0.121355	0.002370	0.094808	
4th-Ventricle	0.613993	0.000000	0.000000	
Brain-Stem	0.001078	0.000001	0.000026	Wilcoxon
CSF	0.716799	0.032999	1	
WM-hypointensities	0.864468	0.085583	1	
Optic-Chiasm	0.001353	0.000000	0.000003	Wilcoxon
$CC_{posterior}$	0.000024	0.000035	0.001418	Wilcoxon
$CC_{Midposterior}$	0.001364	0.000778	0.031139	Wilcoxon
$CC_{Central}$	0.000588	0.168207	1	Wilcoxon
$CC_{MidAnterior}$	0.005830	0.162097	1	Wilcoxon
$CC_{Anterior}$	0.000148	0.042742	1	Wilcoxon
eTIV	0.000000	0.000001	0.000024	Wilcoxon

Table A6. Comparison of FS6 and FS7 aseg volumes in HC group

Volume	Normality differences pval	Comparison pval	Comparison pval Bonferroni	Comment
Left-Lateral-Ventricle	0.000010	0.027409	1	Wilcoxon
Right-Lateral-Ventricle	0.000002	0.002759	0.110365	Wilcoxon
Left-Inf-Lat-Vent	0.170784	0.484447	1	
Right-Inf-Lat-Vent	0.924769	0.757882	1	
Left-Cerebellum-White-Matter	0.000003	0.654464	1	Wilcoxon
Right-Cerebellum-White-Matter	0.000267	0.765542	1	Wilcoxon
Left-Cerebellum-Cortex	0.000000	0.000087	0.003488	Wilcoxon
Right-Cerebellum-Cortex	0.000000	0.000024	0.000971	Wilcoxon
Left-Thalamus	0.001678	0.404681	1	Wilcoxon
Right-Thalamus	0.000009	0.717209	1	Wilcoxon
Left-Caudate	0.000003	0.115452	1	Wilcoxon
Right-Caudate	0.000066	0.062292	1	Wilcoxon
Left-Putamen	0.000045	0.079760	1	Wilcoxon
Right-Putamen	0.000002	0.229707	1	Wilcoxon
Left-Pallidum	0.514772	0.134525	1	
Right-Pallidum	0.167370	0.875284	1	
Left-Hippocampus	0.000027	0.898341	1	Wilcoxon
Right-Hippocampus	0.000015	0.284263	1	Wilcoxon
Left-Amygdala	0.000079	1.000000	1	Wilcoxon
Right-Amygdala	0.000010	0.027409	1	Wilcoxon
Left-Accumbens	0.627203	0.749799	1	
Right-Accumbens	0.241744	0.356982	1	
Left-VentralDC	0.000921	0.005566	0.222641	Wilcoxon
Right-VentralDC	0.000002	0.091958	1	Wilcoxon
Left-vessel	0.117928	0.751045	1	
Right-vessel	0.000706	0.210414	1	Wilcoxon
Left-choroid-plexus	0.032718	0.550352	1	Wilcoxon
Right-choroid-plexus	0.030553	0.522131	1	Wilcoxon
3rd-Ventricle	0.001628	0.083676	1	Wilcoxon
4th-Ventricle	0.000000	0.000012	0.000477	Wilcoxon
Brain-Stem	0.000000	0.000068	0.002737	Wilcoxon
CSF	0.000111	0.091958	1	Wilcoxon
WM-hypointensities	0.000000	0.075989	1	Wilcoxon
Optic-Chiasm	0.790516	0.023392	0.935677	
$CC_{posterior}$	0.000000	0.004788	0.191519	Wilcoxon
$CC_{Midposterior}$	0.000911	0.137330	1	Wilcoxon
$CC_{Central}$	0.136729	0.468354	1	
$CC_{MidAnterior}$	0.363828	0.492248	1	
$CC_{Anterior}$	0.001463	0.017885	0.715396	Wilcoxon
eTIV	0.000000	0.000156	0.006233	Wilcoxon

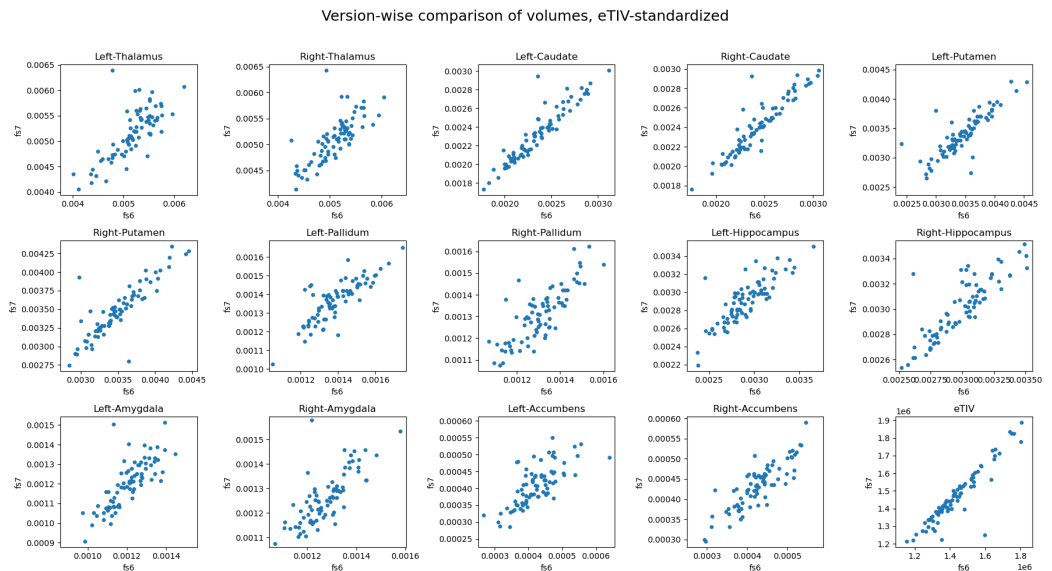Version-wise comparison of volumes, eTIV-standardized

Figure A1. Comparisons between Fressurfer v6.0.1 and v7.4.1 on a selection of volumes

Appendix B

All appendix sections must be cited in the main text. In the appendices, Figures, Tables, etc. should be labeled, starting with "A"—e.g., Figure A1, Figure A2, etc.

References

51. Author 1, T. The title of the cited article. *Journal Abbreviation* **2008**, *10*, 142–149.

52. Author 2, L. The title of the cited contribution. In *The Book Title*; Editor 1, F., Editor 2, A., Eds.; Publishing House: City, Country, 2007; pp. 32–58.

53. Author 1, A.; Author 2, B. *Book Title*, 3rd ed.; Publisher: Publisher Location, Country, 2008; pp. 154–196.

54. Author 1, A.B.; Author 2, C. Title of Unpublished Work. *Abbreviated Journal Name* year, *phrase indicating stage of publication (submitted; accepted; in press)*.

55. Author 1, A.B. (University, City, State, Country); Author 2, C. (Institute, City, State, Country). Personal communication, 2012.

56. Author 1, A.B.; Author 2, C.D.; Author 3, E.F. Title of presentation. In Proceedings of the Name of the Conference, Location of Conference, Country, Date of Conference (Day Month Year); Abstract Number (optional), Pagination (optional).

57. Author 1, A.B. Title of Thesis. Level of Thesis, Degree-Granting University, Location of University, Date of Completion.

58. Title of Site. Available online: URL (accessed on Day Month Year).

TODO (2024-11-22)

1. Revisit and adjust text, tables, and figures 26/11 (Arvid, Astri, Dani)
2. Revisit references 26/11 (Julie, Ben)
3. Consider application for and extension .... (Arvid)
4. Number of participants is fixed to 78
5. A, B, ... D accompanies by a few sentences (Dani)
6.